中國醫藥大學營養學系碩士班

碩士論文

穿心蓮內酯對腫瘤壞死因子誘發 EA.hy926 細胞中細胞黏著分子表現之影響

Effect of andrographolide on tumor necrosis factor-alpha-induced intercellular adhesion molecule-1 expression in EA.hy926 cells

研究生：蔡伊婷 撰 I-Ting Tsai

指導教授：陳暉雯 博士 Haw-Wen Chen, Ph.D.

中華民國九十九年七月

目錄

圖目錄

第一部分

第二部分

表目錄

第一部分

縮寫表

A23187	calcimycin
AC	adenylyl cyclase
ACP	acid phosphatase
AGE	advanced glycation end-product
ALP	alkaline phosphatase
AP	andrographolide
BHC	hexachlorocyclohexane
CAM	cellular adhesion molecule
cAMP	adenosine 3',5' cyclic monophosphate
CAT	catalase
CBP	cAMP respose element binding protein binding protein
Cdk	cyclin-dependent kinase
COX-2	cyclooxygenase-2
CRE	cAMP respose element
CREB	cAMP response element-binding protein
CTL	cytotoxic T lymphocyte
CYP	cytochrome P450 superfamily
ERK1/2	extracellular signal-regulated kinase1/2
fMLP	N-formyl-methionyl-leucyl-phenylalanine
gamma-GTP	gamma-glutamyl transpeptidase
G-CSF	granulocyte colony-stimulating factor
GM-CSF	granulocyte macrophage colony-stimulating factor
GOT	glutamate oxaloacetate transaminase
GPT	glutamate pyruvate transaminase
GR	glutathione reductase
GSH	glutathione
GSH-Px	glutathione peroxidase
GST	glutathione-*S*-transferase
ICAM	intercellular adhesion molecule
Ig	immunoglobulin
IκB	κB inhibitor
IKK	IκB kinase
IL	interleukin
iNOS	inducible NO synthase

KID	kinase-inducible activation domain
LDH	lactate dehydrogenase
LDL	low-density lipoprotein
LOX-1	lectin-like oxidized low-density lipoprotein receptor-1
LPS	lipopolysaccharide
LTB4	leukotriene B4
Mac-1	macrophage adhesion molecule-1
MAPK	mitogen-activated protein kinase
MMP-7	matrix metalloproteinase-7
NEMO	NF-κB essential modulator
NF-κB	nuclear factor-kappa B
NSL	nuclear localization sequence
ox-LDL	oxidized-low-density lipoprotein
PAF	platelet-activating factor
PDE3	Type Ⅲ phosphodiesterase
PECAM-1	platelet endothelial cellular adhesion molecule-1
PGE2	prostaglandin E2
PKA	cAMP-dependent protein kinase
PKC	protein kinase C
PSGL-1	P-selectin glycoprotein ligand
RAGE	receptor for advanced glycation end-products
RHD	Rel-homology domain
ROS	reactive oxygen species
SOD	superoxide dismutase
TNF-α	tumor necrosis factor-α
TXB2	thromboxane B2
VCAM-1	vascular cell adhesion molecule-1
VEGF	vascular endothelial growth factor
VLA-4	very late antigen 4

中文摘要

許多研究顯示，發炎反應及血管內皮細胞功能異常為動脈粥狀硬化起始的關鍵。腫瘤壞死因子 (tumor necrosis factor-α, TNF-α) 為重要的促發炎細胞激素，它會促進內皮細胞中黏著分子的表現，使單核球黏附至內皮細胞上，進而形成動脈粥狀硬化斑塊。穿心蓮 (*Andrographis paniculata*) 中的活性成分穿心蓮內酯 (andrographolide) 被證實具有抗發炎作用。本研究以人類內皮細胞EA.hy926來探討穿心蓮內酯對腫瘤壞死因子所誘發的細胞黏著分子−1 (intercellular adhesion molecule, ICAM-1) 基因表現之影響。研究結果發現，穿心蓮內酯除了能抑制腫瘤壞死因子所誘發的ICAM-1 mRNA、蛋白質及其在細胞膜表面之表現，亦能抑制腫瘤壞死因子所誘發EA.hy926細胞與單核球HL-60細胞的黏附作用。進一步探討發現，穿心蓮內酯會降低腫瘤壞死因子所誘發的κB inhibitor (IκB) kinase (IKK) 及IκBα活化、減少p65進入細胞核內、降低NF-κB與DNA的結合，並且減少ICAM-1報導基因活性。另外研究結果發現，穿心蓮內酯能增加胞內cAMP濃度並活化cAMP response element-binding protein (CREB)，但在knockdown CREB的表現下，穿心蓮內酯抑制腫瘤壞死因子所誘發的ICAM-1表現並不受影響。本研究證實在EA.hy926細胞中，穿心蓮內酯會藉由減少NF-κB活化，進而抑制腫瘤壞死因子所誘發的ICAM-1表現。此研究結果意謂穿心蓮具有預防動脈粥狀硬化發生的潛力。

關鍵字：穿心蓮內酯、腫瘤壞死因子、細胞間黏著分子-1、nuclear factor-kappa B (NF-κB)、EA.hy926 cells

英文摘要

Several lines of evidence indicate that inflammation and endothelial cell dysfunction are important initiating events in atherosclerosis. Tumor necrosis factor-α (TNF-α), a proinflammatory cytokine, induces the expression of cell adhesion molecules and results in monocyte adherence and atheromatous plaques formation. Andrographolide (AP) is a major bioactive diterpene lactone in *Andrographis paniculata*, which possesses anti-inflammatory property. In the present study, we investigated the effect of AP on TNF-α-induced ICAM-1 expression in EA.hy926 cells. AP inhibited TNF-α-induced ICAM-1 mRNA, total protein, and cell-surface expressions. In addition, TNF-α-induced adhesion of HL-60 to EA.hy926 cells was abolished by AP. Furthermore, AP suppressed TNF-α-induced κB inhibitor (IκB) kinase (IKK) and IκBα activation, p65 nuclear translocation, NF-κB and DNA binding activity, and promoter activity of ICAM-1. AP increased intracellular cAMP concentration and induced the phosphorylation of cAMP response element-binding protein (CREB). Transfection with CREB-specific small interfering RNA knocked down CREB expression, however, did not inhibit ICAM-1 expression by AP. Taken together, these results suggest that AP down-regulates TNF-α-induced ICAM-1 expression via attenuation of activation of NF-κB in EA.hy926 cells. The results may implicate the cardiovascular-protective potential of AP.

Keywords：andrographolide; tumor necrosis factor-α; intercellular adhesion molecule-1; nuclear factor-kappa B; EA.hy926 cells

第一部分

第一章 前言

現代人飲食精緻，常攝取過多油脂，易罹患心血管慢性疾病。依據行政院衛生署統計資料顯示，在國人十大死因當中心臟疾病與腦血管疾病近年來逐步攀升至前三名僅次於惡性腫瘤 (行政院衛生署，2009)，可見心血管疾病日趨嚴重。氧化型低密度脂蛋白的累積或血管內皮的損傷將造成血管內皮細胞功能異常，促進細胞激素及黏著分子的表現。長期白血球的過度徵募會促使動脈粥狀硬化斑塊與脂肪條紋的生成，造成動脈粥狀硬化的發生，進一步可能導致局部缺血或梗塞等嚴重的後果 (Hansson, 2005, 2009)。

除了亞洲國家以外，傳統應用於保健預防或疾病治療的中草藥也逐漸受到西方國家的重視，而這些中草藥當中的有效成分及其作用機轉更備受矚目。穿心蓮在傳統醫療上多用來治療感冒發熱、咽喉腫痛等，具有清熱解毒之效。在過去的文獻當中指出穿心蓮具有抗發炎的作用 (Abu-Ghefreh et al., 2009; Bao et al., 2009)，而動脈粥狀硬化即為慢性發炎的疾病之一，因此本研究將以內皮細胞所表現的細胞黏著分子為指標，探討穿心蓮內酯對其之影響及其所透過的分子機制，以期望使穿心蓮的預防保健功效更為清楚。

第二章 文獻探討

一、穿心蓮

在許多亞洲國家傳統中草藥廣泛的應用於日常生活中，除了替代藥物用以治療疾病外亦可入膳用於預防保健。隨著養生觀念受到重視，中草藥的應用除了亞洲地區之外亦逐漸受到西方國家的重視。因此關於這些藥用植物的研究也越來越多，進而使其功效、活性成分及作用機轉一一逐步釐清。

穿心蓮，拉丁學名*Andrographis paniculata* (Burm. f.) Nees，它屬於爵床科 (Acathaceae)、穿心蓮屬 (*Andrographis*)，又名一見喜、苦膽草、印度草、斬蛇劍等。穿心蓮生長主要分布於印度、斯里蘭卡、泰國、越南等東南亞熱帶地區，另外中國大陸與台灣各地也有零星栽培。穿心蓮為一年生草本植物，主要於夏秋兩季割取地上部分，曬乾後以水煎熬服用。穿心蓮性苦味寒，具清熱解毒之效，於傳統醫療應用上多用以治療感冒發熱、咽喉腫痛、口舌生瘡及毒蛇咬傷等。目前研究發現穿心蓮具有多種生理功效，包括抗發炎 (Abu-Ghefreh et al., 2009; Bao et al., 2009)、抗癌 (Jiang et al., 2007; Rajagopal et al., 2003; Zhao et al., 2008)、保護肝臟 (Trivedi et al., 2007)、抗病毒 (Chen et al., 2009)、抗氧化 (Akowuah et al., 2008) 及降血糖 (Yu et al., 2003; Zhang and Tan, 2000) 等。研究指出穿心蓮的活性成分主要包括diterpenes、flavonoids及polyphenols。目前已知的diterpenes有andrographolide，neoandrographolide，14-deoxy-ll, 12-dihydroandrographolide，14-deoxyandrographolide，14-deoxy-11-hydroxyandrographolide及12-didehydro-andrographolide等；flavonoids包括7-O-methylwogonin，dihydroskullcapflavone I，

7-O-methyldihydrowogonin，5-hydroxy-7,8,20,50-tetramethoxy-flavone，5-hydroxy-7,8,20,30-tetramethoxyflavone和5-hydroxy-7,20,60-trimethoxyflavone等；而polyphenols則包括cinnamic acid，caffeic acid，ferulic acid及chlorogenic acid等 (Koteswara Rao et al., 2004)。在這些已知的diterpenes中，穿心蓮內酯 (andrographolide) 是最受重視的活性成分，其結構式：3-[2-[decahydro-6-hydroxy-5-(hydroxymethyl)-5,8a- dimethyl-2-methylene-1-napthalenyl]ethylidene]dihydro- 4-hydroxy-2(3H)-furanone，分子式：$C_{20}H_{30}O_5$，分子量為350.45，主要存在於穿心蓮葉子當中。以高效能液相層析法 (high performance liquid chromatography, HPLC) 分析穿心蓮葉子的乙醇萃取物，每公克乾燥的葉子含有44.48毫克穿心蓮內酯 (Wongkittipong et al., 2004)。

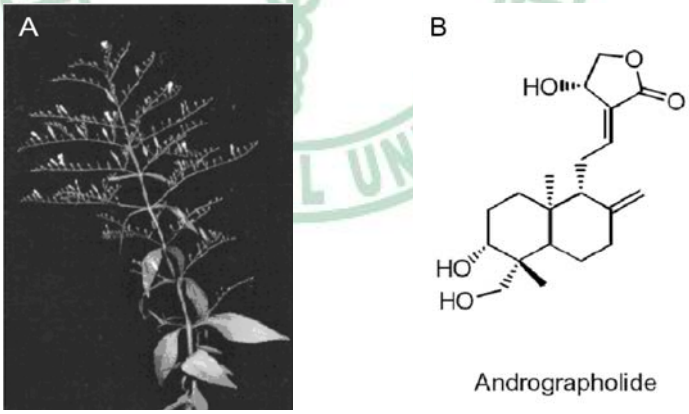

圖 2.1 (A)穿心蓮 (Singha et al., 2007)，(B)穿心蓮內酯結構 (Satyanarayana et al., 2004)

1. 穿心蓮功效

1.1 穿心蓮抗發炎作用

過去的文獻指出，穿心蓮萃取物可明顯減輕上呼吸道感染的症狀及降低感冒的發生率 (Coon and Ernst, 2004; Poolsup et al., 2004)，推測可能與穿心蓮內酯具有解熱、抗發炎及免疫調節等作用有關。在 Spasov 等人 (2004) 的研究中更證實了兒童在上呼吸道感染期間合併服用穿心蓮萃取物可明顯縮短痊癒時間並減少鼻分泌物中的 interleukin (IL) -6 和 immunoglobulin (Ig) A。另外，還有相當多的研究探討穿心蓮抗發炎作用。Chandrasekaran 等人 (2010) 的研究中指出以白血球細胞為實驗模式，證實穿心蓮葉子的萃取物可負向調控由 lipopolysaccharide (LPS) 或 calcimycin (A23187) 所誘發的發炎或過敏相關的介質產生，包括一氧化氮 (nitric oxide，NO)、prostaglandin E_2 (PGE_2)、IL-1β、IL-6、leukotriene B_4 (LTB_4) 及 thromboxane B_2 (TXB_2)。在鼠科類巨噬細胞 RAW264.7 細胞株中穿心蓮內酯可透過抑制 inducible NO synthase (iNOS) 的表現來減少由 LPS 所誘發的 NO 產生 (Chiou et al., 2000)。利用 LPS 刺激小鼠腹膜巨噬細胞模式下，穿心蓮內酯可藉由抑制 ERK1/2 磷酸化，減少 tumor necrosis factor-α (TNF-α) 及 IL-12 的產生 (Chiou et al., 2000; Qin et al., 2006)。當以 ovalbumin 誘發 BALB/c 小鼠產生過敏性氣喘時，給與穿心蓮內酯具有降低發炎反應的作用 (Li et al., 2009)，包括降低呼吸道細胞浸潤、減少支氣管灌流液中的細胞激素 (cytokines) 與趨化細胞激素 (chemokines) 表現量等，而此作用跟降低 nuclear factor-κB (NF-κB) translocation 及抑制 NF-κB 與 DNA 的結合有關 (Bao et al., 2009)。此外，體外試驗模式也發現以 platelet-activating factor (PAF) 或 N-formyl-methionyl-leucyl-phenylalanine (fMLP) 刺激白血球細胞 HL-60，穿心蓮內酯並不影響 mitogen-activated protein kinase (MAPK) 路徑及 inhibitor-κB (IκB) α 的降解，而是透過抑制 NF-κB 與 DNA 的結

合來降低前發炎蛋白質 cyclooxygenase-2 (COX-2) 的表現 (Hidalgo et al., 2005)。相反地，有研究指出穿心蓮內酯可透過抑制 extracellular signal-regulated kinase1/2 (ERK1/2) 路徑來抑制 thrombin 所誘發的血小板凝集 (Thisoda et al., 2006)。而在以 fMLP 刺激人類白血球細胞的模式中發現，穿心蓮內酯可透過調控 protein kinase C (PKC) 路徑減少 reactive oxygen species (ROS) 的產生，進一步降低 macrophage adhesion molecule-1 (Mac-1)表現而達到抑制白血球的黏附作用及血球滲入血管壁 (transmigration) (Shen et al., 2002)。上述研究顯示，穿心蓮內酯透過調控訊息傳遞路徑或影響轉錄因子活性來抑制細胞激素、趨化細胞激素及其他發炎相關蛋白質的表現進而達到抗發炎的作用。

1.2 穿心蓮抑制腫瘤生長作用

近年來有許多研究顯示穿心蓮具有抗癌的作用，包括胃癌、肝癌、肺癌及乳癌等，其中參與的機制可能包含了誘發癌細胞凋亡、促使細胞週期停滯或增加淋巴球細胞的抗癌活性 (Qi et al., 2007) 等。在 Rajagopal等人 (2003) 的研究中利用包括乳房、結腸、卵巢、肺、前列腺、腎臟等多種癌細胞株證實穿心蓮內酯能抑制癌細胞的生長，且體外試驗中發現穿心蓮內酯亦可促進人類週邊血液淋巴球增生與增加淋巴球對K562癌細胞株細胞溶解 (cytolytic) 作用。Sheeja 和 Kuttan (2007) 的研究觀察到在殖入B16F-10黑色素瘤細胞株的C57BL/6小鼠中穿心蓮萃取物及穿心蓮內酯能調控cytokines的表現，且無論是在體內或體外試驗皆能促進cytotoxic T lymphocyte (CTL) 的產生，可能藉此達到抑制腫瘤生長、延長動物生命期的作用。另外也有研究發現穿心蓮內酯可降低非小細胞肺癌A549細胞的移行與侵襲作用，而此作用可能與穿心蓮內

酯抑制PI3K/Akt/AP-1訊息傳遞路徑來降低matrix metalloproteinase-7 (MMP-7) 基因表現有關 (Lee et al., 2010)。關於前列腺癌，穿心蓮內酯則是透過活化caspase 3、增加bax表現、抑制bcl-2與vascular endothelial growth factor (VEGF) 表現等作用來誘發前列腺癌 (prostate cancer-3) 細胞凋亡 (Zhao et al., 2008)。除了體外試驗，利用將癌細胞株植入動物體內的模式來探討穿心蓮對抑制腫瘤生長的研究亦多。無論以MCF7乳癌細胞株的體外試驗或將MCF7植入Swiss Albino小鼠的腹膜與皮下的體內試驗都發現穿心蓮內酯可透過誘發蛋白p27 (它可抑制細胞週期)表現與減少cyclin-dependent kinase (Cdk) 4而促使細胞週期停滯於G0-G1期 (Satyanarayana et al., 2004)。在植入B16F-10黑色素瘤細胞的C57BL/6小鼠實驗中也發現，無論給與穿心蓮萃取物或穿心蓮內酯都可以降低由黑色素瘤細胞所誘發的血管新生作用，其中除了透過抑制前發炎細胞激素及一氧化氮產生外也會減少VEGF的生成 (Sheeja et al., 2007)。這些相關的研究證實穿心蓮內酯能直接影響癌細胞增生、促進癌細胞凋亡或間接透過調控免疫活性來產生抗癌的作用。

1.3 穿心蓮肝臟保護作用

許多研究顯示穿心蓮及穿心蓮內酯對於carbon tetrachloride、hexachlorocyclohexane (BHC)、ethanol或paracetamol所造成的肝臟毒性傷害具有保護作用 (Maiti et al., 2010; Trivedi et al., 2007, 2009; Visen et al., 1993)。在動物實驗中發現穿心蓮內酯可對抗由carbon tetrachloride所誘發的肝損傷，包括降低血漿中glutamate oxaloacetate transaminase (GOT)、glutamate pyruvate transaminase (GPT)、alkaline phosphatase (ALP)和lactate dehydrogenase (LDH) 等指標性酵素與bilirubin的含量 (Maiti

et al., 2010)。利用BHC誘發肝腫瘤產生的模式，評估穿心蓮內酯對肝臟抗氧化防禦系統的影響，發現穿心蓮內酯會增加glutathione (GSH) 含量與glutathione reductase (GR)、glutathione peroxidase (GSH-Px)、superoxide dismutase (SOD)、catalase (CAT) 活性，降低glutathione-*S*-transferase (GST) 與gamma-glutamyl transpeptidase (gamma-GTP) 活性 (Trivedi et al., 2007)。在小鼠試驗中發現除了穿心蓮內酯，從穿心蓮中所萃取出來的arabinogalactan proteins亦具有抗酒精誘發肝毒性的作用，兩種成分皆可抑制由酒精毒性所誘發的GOT、GPT、acid phosphatase (ACP) 及lipid peroxidation (Singha et al., 2007)。大鼠初代肝細胞實驗發現穿心蓮內酯可能透過增加胞內adenosine 3',5' cyclic monophosphate (cAMP)、活化cAMP response element-binding protein (CREB)來調控 π class GST表現 (Yang et al., 2010)。

2. 穿心蓮使用風險

藥物或外來毒物在人體內可由肝臟經其生物轉換酵素系統作用後將藥物或毒素代謝排出體外，而穿心蓮除了先前提到可增加肝臟抗氧化防禦系統的活性外，亦可調控生物轉換酵素系統的表現 (Jaruchotikamol et al., 2007; Pekthong et al., 2009; Pekthong et al., 2008)。穿心蓮對於cytochrome P450 superfamily (CYP) 的影響並沒有定論，Jaruchotikamol等人 (2007) 在小鼠初代肝細胞的研究中發現穿心蓮內酯會誘發CYP1A1與CYP1A2的基因表現；Pekthong等人 (2009; 2008) 指出給予大鼠穿心蓮萃取物及穿心蓮內酯會顯著抑制肝臟微粒體CYP2C11的活性，而在人類或大鼠肝細胞中穿心蓮萃取物及穿心蓮內酯對CYP1A2、CYP2C及CYP3A4等的活性也有不等程度的抑制作用。基於以上實驗數據，有一點值得特別注意，同時攝取

穿心蓮及藥物時可能會產生herb-drug interactions，因為當這些CYP表現及活性改變時會導致促進或抑制藥物與毒物的代謝作用。

另外，評估穿心蓮對雄性動物生殖功能的影響時發現，給予雄性SD大鼠每天每公斤體重1000 mg的穿心蓮萃取物六十天對其睪丸組織、Leydig cells並無異常作用同時對testosterone的分泌並無影響 (Burgos et al., 1997)。但在Akbarsha等人 (1990) 的研究中卻發現穿心蓮可能含有抗雄性激素作用的成分會對雄性動物的生殖功能造成影響。進一步研究發現當給予雄性Wistar大鼠每天每公斤體重50 mg穿心蓮內酯為期四十八天後發現會減少精子的產生、降低精子泳動能力，並造成副睪、輸精管的退化 (Akbarsha and Murugaian, 2000)。在利用Ames test評估穿心蓮萃取物的致基因突變實驗中證實16~5000 μg/mL穿心蓮萃取物不會造成基因突變；而急性毒性試驗方面則證實給予雌性大鼠每公斤體重口服5000 mg的穿心蓮萃取物十四天並未造成急性毒性反應 (Chandrasekaran et al., 2009)。Guo等人 (1988) 指出每日餵食小鼠每公斤體重500 mg的穿心蓮為期十天並不會影響小鼠的生長、食慾與糞便型態等，且當白兔予以靜脈注射每公斤體重10 mg穿心蓮內酯後檢測其心血管、肝臟酵素、心臟、肝臟、腎臟及脾臟皆無異常。

二、動脈粥狀硬化

1. 動脈粥狀硬化之成因

依據行政院衛生署統計資料顯示，自民國七十五年起至民國九十七年為止心臟疾病及腦血管疾病皆位居十大死因的前四名，尤其近年來更是逐步攀升至前三名僅次於惡性腫瘤 (行政院衛生署, 2009)，足見心血管疾病之嚴重性。動脈粥狀硬化是慢性發炎疾病，其相關的危險因子包括高血壓、糖尿病、抽菸及血清膽固醇增加等，尤其是血中低密度脂蛋白

(low-density lipoprotein，LDL) 增加被認為是最重要的危險因子。血管內皮層下的氧化型低密度脂蛋白 (oxidized-low-density lipoprotein，ox-LDL) 累積或血管壁損傷皆會活化內皮細胞，而內皮細胞功能異常將會促進前發炎細胞激素或趨化細胞激素的分泌與黏著分子的表現，造成白血球 (leukocytes)，包括單核球及T-cells 的過度徵募。進入血管壁內之單核球會分化成巨噬細胞增加scavenger receptors與toll-like receptors等的表現，促進對ox-LDL的汲取 (uptake) 進而形成泡沫細胞 (foam cell) 與增加細胞激素、蛋白質酶及vasoactive molecules等的釋出 (圖2.2A)；T-cells則會促進前發炎細胞激素分泌 (圖2.2B)。上述這些作用都將促進斑塊 (plaque) 的生長 (圖2.3)，包括加強發炎細胞的徵募作用及平滑肌細胞的增生，進而形成脂肪條紋 (fatty streak)。進一步將促使局部蛋白質水解、斑塊破裂及血栓形成，最後導致局部缺血及梗塞 (Hansson, 2005, 2009)。

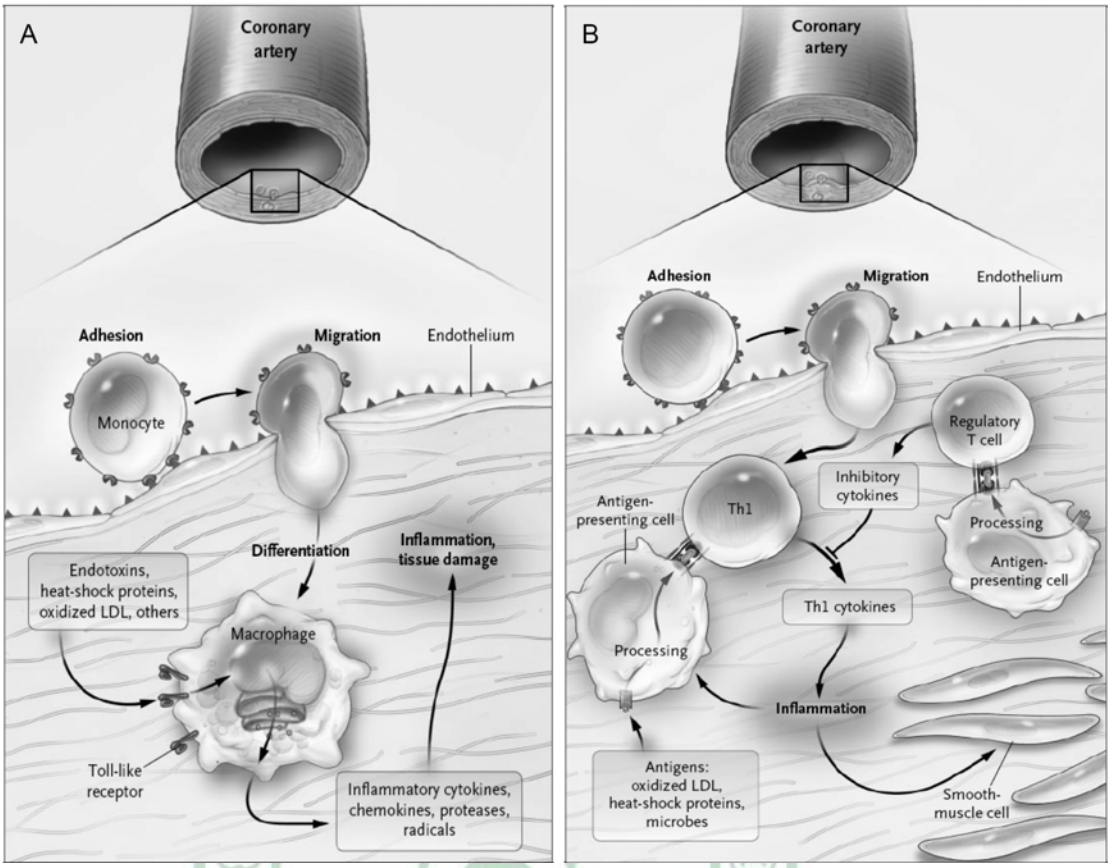

圖 2.2 白血球(A)單核球 (B)T-cells 對動脈粥狀硬化形成之影響 (Hansson, 2005)

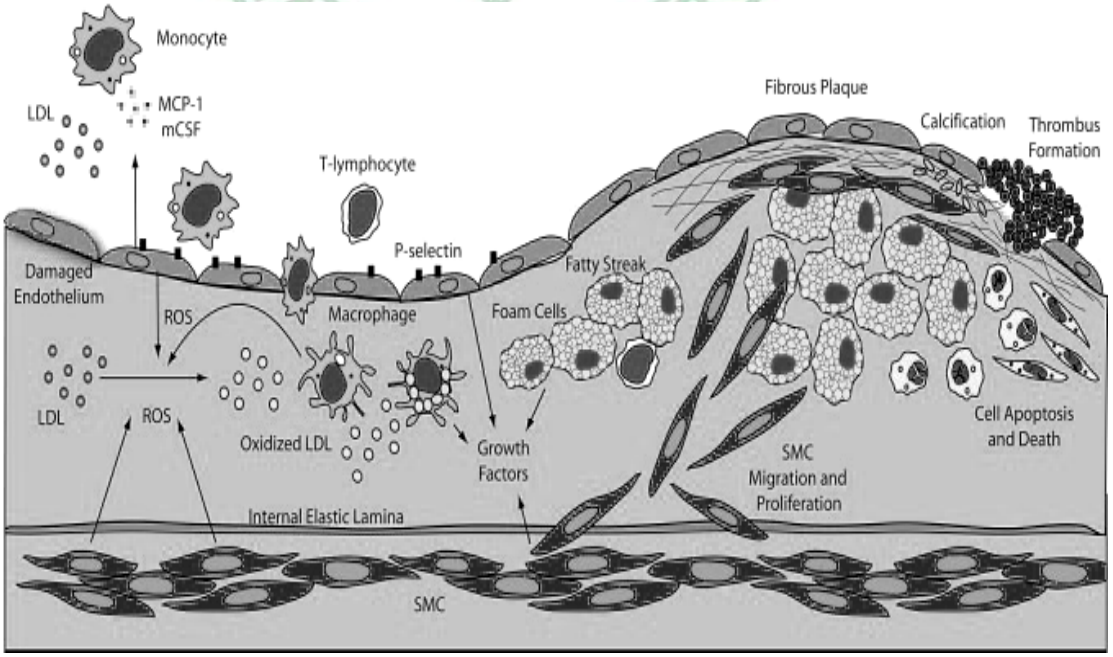

圖2.3 動脈粥狀硬化之形成 (Madamanchi et al., 2005)

2. 白血球徵募作用

動脈粥狀硬化損傷形成的最初期步驟是白血球的徵募作用 (recruitment)，而黏著分子及細胞激素在這過程中扮演重要的角色。白血球的徵募作用 (圖2.4) 主要包括下列步驟：(1)透過與選擇素 (selectins) 的交互作用使白血球產生tethering及滾動 (rolling)；(2)透過細胞激素活化白血球細胞表面的整合素 (integrins)，改變整合素的構型以促進其與ligands的黏附；(3)白血球spreading並藉由類免疫球蛋白 (Immunoglobin-like molecules) 與整合素的交互作用穩固地附著在內皮上；(4)白血球由內皮層滲透至內皮層下，進而造成後續反應促使動脈粥狀硬化的形成 (Lawson and Wolf, 2009)。

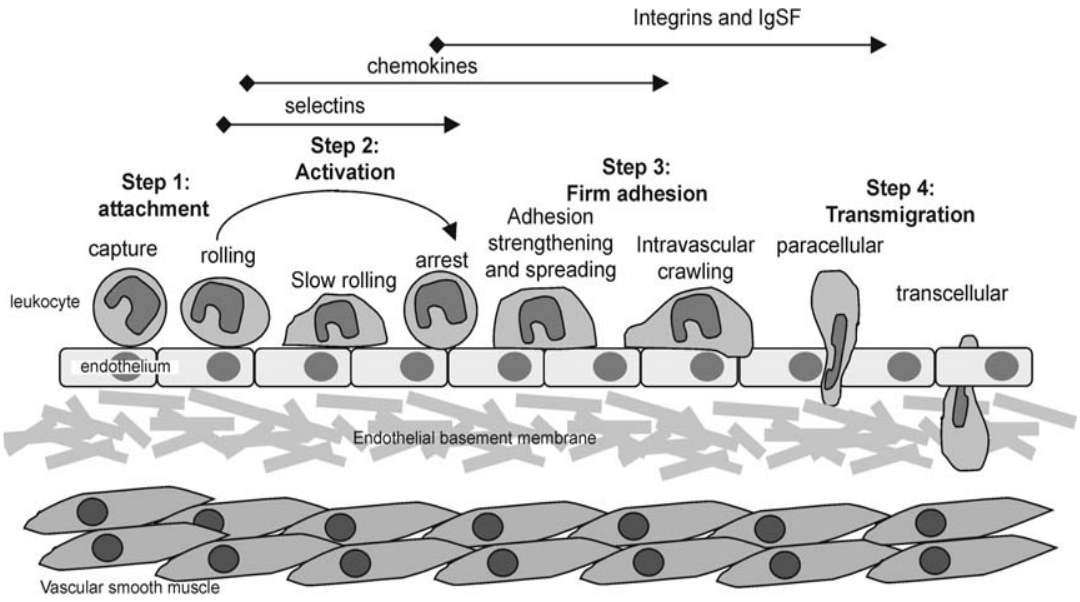

圖 2.4 白血球徵募作用 (Lawson and Wolf, 2009)

2.1 黏著分子

在動脈粥狀硬化形成的過程中各種黏著分子分別參與了白血球的 tethering、滾動、黏附及滲透至血管壁內的過程 (Galkina and Ley, 2007)。以免疫組織化學 (immunohistochemistry) 染色影像證實在動脈產生動脈粥狀硬化斑塊的區域有黏著分子的表現 (Kaufmann et al., 2007)。而依據 Gene Ontology Consortium 定義，細胞黏著分子為表現於細胞表面之分子且調控與其他細胞或胞外基質的黏附作用，大致可分為三類，包括選擇素、類免疫球蛋白分子及整合素 (表 2.1) (Blankenberg et al., 2003)。

表 2.1 黏著分子及其配體 (Blankenberg et al., 2003)

Adhesion molecules	Other names	Ligands	Functions	Tissue distribution			Soluble form
				Endoth	Leuko	Platelets	
Selectins/ligands							
P-selectin	CD62P, GMP140	PSGL-1, Lewis X, CD24	Rolling/tethering	+		+	+
E-selectin	CD62E, ELAM1	ESL-1, Lewis X, PSGL-1, L-set	Rolling/tethering	+			+
L-selectin	CD62L	Lewis X, CD34, PSGL-1, GlyCAM	Rolling/tethering		+		+
E-selectin ligand 1	ESL-1	E-selectin	Rolling/tethering		+		
P-selectin ligand 1	CD162, PSGL-1	P-, L-, E-selectin	Rolling/tethering		+		+
Immunoglobulins							
ICAM-1	CD54	αLβ2, αMβ2, αXβ2	Firm adhesion	+	+		+
ICAM-2	CD102	αLβ2, αMβ2	Firm adhesion	+	+	+	+
ICAM-3	CD50	αLβ2, αDβ2, DC-SIGN	Firm adhesion	+	+		+
VCAM-1	CD106	α4β1, α4β7, αDβ2	Firm adhesion	+			+
PECAM-1	CD31	PECAM-1, αVβ3	Endothelial integrity, leukocyte extravasation	+	+	+	+
Integrins							
Integrin α2/β1	CD49b/CD29, VLA2	Collagen, laminin	Platelet receptor			+	
Integrin α4/β1	CD49d/CD29, VLA4	VCAM-1, FN	Firm adhesion	+			
Integrin αL/β2	CD11a/CD18, LFA1	ICAMs	Firm adhesion		+		
Integrin αM/β2	CD11b/CD18, Mac1	ICAMs,iC3b, FX, FG	Firm adhesion		+		
Integrin αX/β2	CD11c/CD18	ICAM-1, FG, iC3b, CD23	Firm adhesion		+		
Integrin αD/β2	CD11d/CD18	ICAM-3, VCAM-1	Firm adhesion		+		
Integrin α2B/α3	GPIIb/IIIa	vWF, FN, FG, VN, thrombospondin	Platelet receptor			+	
Integrin αV/β3	VNR, CD51/CD61	PECAM-1, VN, FN, FG, vWF	Proliferation, migration	+		+	
Integrin αV/β5		VN	Proliferation, migration	+			

2.1.1 選擇素 (selectins)

選擇素主要參與調控白血球在內皮層的 tethering 與滾動，包括 L-selectin、P-selectin 及 E-selectin。選擇素與其配體 (ligand) 產生交互作用，促使血流中的白血球降低流動速度以利後續黏附於活化的內皮細胞之作用。

L-selectin 主要表現於白血球，在 L-selectin 缺陷之淋巴球研究中證實 L-selectin 表現減少時會降低 50%淋巴球在主動脈上的移行作用 (Galkina et al., 2006)。P-selectin glycoprotein ligand (PSGL-1) 為 L-selectin 的配體之一，廣泛的存在嗜中性球、單核球與淋巴球，透過 L-selectin 與 PSGL-1 的結合會促使血液循環當中的白血球與在血管內皮上滾動的白血球產生交互作用，促進 secondary capture 的發生。有研究指出 L-selectin 調控白血球的徵募作用可能主要是藉由 L-selectin/PSGL-1 影響 secondary capture (Eriksson et al., 2001)。此外，PSGL-1 亦是 P-selectin 或 E-selictin 的配體，小鼠單核球 Ly-6C^{hi} 就是透過高度表現 PSGL-1 而增加與 L-、P-及 E-selectin 的結合，降低白血球滾動的速度，促使動脈粥狀硬化損傷發生 (Hung et al., 2008)。

P-selectin 主要儲存於血小板的 α-granules 中，但在內皮細胞的 Weibel-Palade bodies 中也有，一旦內皮細胞活化後便迅速釋放至細胞膜表面。研究顯示當以乙醛刺激內皮細胞時，利用 P-selectin 抗體阻斷 P-selectin 的作用或利用 siRNA 抑制 P-selectin 的表現皆會顯著降低由乙醛所誘發的單核球 THP-1 黏附作用 (Redmond et al., 2009)。

E-selectin 則只有表現於內皮細胞，在非發炎反應的情況下不

會表現，必須受到發炎細胞激素如 IL-1 或 TNF-α 等的刺激才會誘發其轉錄作用促進 E-selectin 合成，而轉錄因子 NFκB 與此基因表現有關 (Lin et al., 2007; Zakeri et al., 2000)。

2.1.2 類免疫球蛋白分子 (Immunoglobin-like molecules)

類免疫球蛋白分子 superfamily 為表現於細胞膜上的醣蛋白，而這些基因透過不同的剪接作用 (splicing) 產生多種 isoforms。

Intercellular adhesion molecules (ICAM) 屬於此 superfamily 中的次家族，包括五個成員，ICAM-4 表現於 erythroid cells，ICAM-5 表現於大腦，與動脈粥狀硬化較無相關。ICAM-1 廣泛的表現於白血球與內皮細胞，在前發炎細胞激素的刺激下更會大量的表現；ICAM-2 表現於白血球、血小板及內皮細胞，受發炎細胞激素的負向調控；ICAM-3 除了表現於白血球與內皮細胞外，更是唯一表現於嗜中性白血球的細胞黏著分子。ICAM 的配體主要是表現於白血球的 β_2 整合素，藉由兩者之間的結合調控白血球的黏附作用，促進白血球穩固的黏附於血管表面，以利白血球滲入血管壁的作用 (Blankenberg et al., 2003)。

Vascular cell adhesion molecule 1 (VCAM-1) 除了表現於內皮細胞外，巨噬細胞、myoblasts 與 dendritic cells 亦會表現。在活化的內皮細胞中，VCAM-1 藉由促使白血球牢固的黏附於內皮而參與白血球的徵募 (Blankenberg et al., 2003)。VCAM-1 會與選擇素 $\alpha_4\beta_1$ (又稱為 very late antigen 4，VLA-4) 作用，誘發內皮細胞的相關訊息，促使其改變形狀以利白血球滲入血管壁下層。研究發現當加入 anti-VCAM-1-coated bead 或 anti-α_4 integrin-coated beads 可

抑制淋巴球的移行作用，顯示淋巴球的移行需要 VCAM-1 的黏附作用 (Matheny et al., 2000)。

另外，platelet endothelial cellular adhesion molecule 1 (PECAM-1) 則表現於白血球、血小板及內皮細胞。在內皮細胞的連接處可觀察到特別密集的 PECAM-1 表現，其主要參與相鄰的細胞之間鍵結，與內皮的完整性和細胞由血管滲入內皮下層有關 (Newton et al., 1997)。

- ICAM-1 (CD54)

ICAM-1 為跨膜的醣蛋白，由 505 個胺基酸組成，不含醣基的分子量約為 60 kDa，而其醣基化程度在不同的細胞有所差異，依其醣基化程度分子量大小約介於 80 到 114 kDa (van de Stolpe and van der Saag, 1996)。ICAM-1 在白血球的徵募作用中透過與整合素產生交互作用，停止白血球的滾動，將白血球穩固地黏附於內皮層。許多研究包括利用抗體阻斷 ICAM-1 的作用或藉由 ICAM-1 缺陷的模式證實 ICAM-1 的黏附作用對於淋巴球穿透內皮層的移行過程相當重要 (Lehmann et al., 2003; Reiss and Engelhardt, 1999)。除了內皮細胞與白血球外，許多細胞包括上皮細胞、平滑肌細胞、纖維母細胞及角質細胞等皆會表現 ICAM-1 (Roebuck and Finnegan, 1999)。ICAM-1 除了與動脈粥狀硬化有關外，它與其他疾病亦有關，如：氣喘 (Cui et al., 2010)、局部缺血再灌流的損傷 (Cheng et al., 2008)、自體免疫疾病 (autoimmune disease) (Yusuf-Makagiansar et al., 2002)等。

人類 ICAM-1 基因位於第十九號染色體，包括七個 exons 與六

個 introns (Voraberger et al., 1991)。在病毒感染、氧化壓力、LPS、ox-LDL 或其他相關的促發炎細胞激素 (如：TNF-α、IL-1、IL-6、IFN-γ 等) 刺激下會誘發 ICAM-1 表現。發炎介質透過調控 MAPK (Ying et al., 2009)、PKC (Min et al., 2005)、JAK/STAT (Audette et al., 2001)、Akt (Oh and Kwon, 2009)及 IKK/NF-κB (Lian et al., 2010) 等訊息傳遞路徑來誘發 ICAM-1 表現。參與調控 ICAM-1 表現的轉錄因子包括 AP-1 (Son et al., 2006)、STAT (Audette et al., 2001)、Sp1 (Berendji-Grun et al., 2001) 與 NF-κB (van de Stolpe and van der Saag, 1996; Zhou et al., 2007) 等。研究指出 ICAM-1 DNA 5'端的數百個鹼基對 (base pairs) 對於前發炎細胞激素誘發 ICAM-1 的表現相當重要 (Hou et al., 1994; van de Stolpe and van der Saag, 1996)。比較位於 ICAM-1 promoter 上的轉錄因子 (包含 AP-1、NF-κB、STAT) 結合位置，當以 TNF-α 刺激內皮細胞時，DNA 序列上的 NF-κB 結合位置對 ICAM-1 的表現相對重要 (Oh et al., 2010)。另有研究指出藉由 forskolin (adenylyl cyclase 活化劑) 增加胞內 cAMP 或利用 cAMP 相似物能夠抑制 TNF-α、IL-1β 或 IFN-γ 所誘發的 ICAM-1 蛋白質與 mRNA 表現 (Balyasnikova et al., 2000; Panettieri et al., 1995)。

2.1.3 整合素 (integrins)

整合素為細胞表面的接受器，由 18 種 α 與 8 種 β 次單元體所組成的 αβ 異質二聚體 (heterodimer) (Hynes, 2002)，調控著包括細胞與細胞、細胞與胞外基質及細胞與病原體之間的接觸。整合素表現於細胞表面，在未活化的細胞中整合素對配體的親合力低，

一旦受到刺激活化便會迅速改變其胞外 domain 的構型，增加對配體的親合力 (Blankenberg et al., 2003)。各種次單元中主要參與白血球黏附作用的是 β_2 與 α_4，LFA-1 (CD11a/CD18, $\alpha_L\beta_2$) 屬於整合素的 β_2 次家族 (subfamily)，在所有的白血球皆會表現，它能夠與免疫球蛋白中的 ICAMs 作用；VLA-4 (CD49d/CD29, $\alpha_4\beta_1$) 則屬於 α_4 次家族，主要表現於單核球與淋巴球，會與 VCAM-1 及 fibronectin 作用 (Galkina and Ley, 2007)。

2.2 細胞激素

活化的內皮細胞、白血球及淋巴球等會釋出許多參與發炎反應的細胞激素，而這些細胞激素會經由其相對的接受器調控訊息傳遞路徑，進而誘發黏著分子表現與促進白血球徵募作用。如表 2.2 所列，許多細胞激素 (包括 TNF-α、IL-1 及 IFN-γ 等) 會誘發細胞黏著分子 (cellular adhesion molecule, CAM) 表現 (Meager, 1999)。

表 2.2 細胞激素誘發細胞黏著分子的表現 (Meager, 1999)

Cytokine	CAM Expression
TNF-α, TNF-β, IL-1α, IL-1β	E-selectin, P-selectin, L-selectin ligand, ICAM-1, VCAM-1, MAdCAM-1 strongly up-regulated.
IL-4, IL-13	Selective up-regulation of VCAM-1 (synergize with TNF-α); late expression of E-selectin stimulated by TNF-α or IL-1 inhibited.
IL-10	Potential inhibitor of TNF-α induced ICAM-1 expression.
IFN-γ	Weak inducer of ICAM-1 expression, but strong synergy with either TNF or IL-1. Can maintain E-selectin expression levels.
TGF-β_1	E-selectin expression inhibited (additive inhibitory effect with IL-4); up-regulation of PECAM-1.

- TNF-α

TNF-α 被認為與動脈粥狀硬化等心臟疾病有關，醣化終產物及

其接受器 (advanced glycation end-products, AGE/receptor for AGEs，RAGE)、lectin-like oxidized low-density lipoprotein receptor-1 (LOX-1) 及 NFκB 等訊息傳遞路徑對於 TNF-α 的表現扮演重要角色 (Gao et al., 2007; Li et al., 2003)。體外試驗中發現 LPS 會透過活化 NF-κB 促進豬左冠狀動脈組織及其平滑肌細胞產生 TNF-α，但在 forskolin 或 cAMP 相似物存在下會增加胞內 cAMP 濃度並抑制由 LPS 所誘發 TNF-α 產生 (Newman et al., 1998)。TNF-α 除了會增加活性氧分子的產生 (Kumar et al., 2007)，造成內皮細胞功能異常外，當內皮細胞在 TNF-α 刺激下，透過活化轉錄因子 NF-κB 亦會促進與發炎相關的基因 (如 ICAM-1、VCAM-1、MCP-1 與 IL-8 等) 表現，並且促使白血球黏附於內皮細胞上 (Kim et al., 2007; Min et al., 2005)。但當人類臍靜脈內皮細胞預先處理 TNF-α 抗體或以 siRNA 抑制 TNF-α 表現皆可顯著減少由乙醛所誘發的單核球 THP-1 黏附作用 (Redmond et al., 2009)。比較 TNF-$\alpha^{-/-}$apoE$^{-/-}$小鼠與 apoE$^{-/-}$小鼠兩者之間的血漿總膽固醇濃度相仿，但 apoE$^{-/-}$小鼠的動脈粥狀硬化損傷程度較為嚴重，且其 ICAM-1、VCAM-1 mRNA 表現皆顯著高於 TNF-$\alpha^{-/-}$apoE$^{-/-}$小鼠 (Ohta et al., 2005)。另外，apoE$^{-/-}$小鼠除了 ICAM-1 與 VCAM-1 外，其他與促進動脈粥狀硬化相關的基因包括 IL-1β、IFN-γ、MCP-1、granulocyte macrophage colony-stimulating factor (GM-CSF) 及 NF-κB (p65) 等 mRNA 表現皆高於 TNF-$\alpha^{-/-}$apoE$^{-/-}$小鼠，而 TNF-$\alpha^{-/-}$apoE$^{-/-}$小鼠的動脈脂肪條紋損傷面積亦明顯減少 (Xiao et al., 2009)。上述相關研究顯示 TNF-α 的表現對於動脈粥狀硬化的形成扮演重要角色。

三、參與發炎反應之訊息傳遞路徑與轉錄因子

1. IκB kinase (IKK)/NF-κB

IKK/ NF-κB路徑參與調控許多生理作用包括免疫反應、細胞死亡與發炎反應。NF-κB為一群轉錄因子的統稱，在哺乳動物細胞中NF-κB包含五個家族成員，分別為RelA (p65)、RelB、c-Rel、p50/p105 (NF-κB1) 與p52/p100 (NF-κB2)。這五個家族成員在N端domain上含有約300個胺基酸的Rel-homology domain (RHD) 對於與抑制蛋白質 (inhibitor-κB，IκB) 及與DNA序列的結合相當重要。RHD亦與NF-κB的五個家族成員互相形成同質或異質二聚體有關，二聚體中以p65/p50異質二聚體最為常見。大部分的NF-κB二聚體與目標基因的啟動子 (promoter) 結合後具有促進基因轉錄的作用，但也有例外，比如p50或p52所形成的同質二聚體卻會抑制轉錄作用。

在未受到刺激的情況下，NF-κB存在於細胞質中與IκB結合，此時IκB會遮蔽RHD上調控轉移作用 (translocation) 的nuclear localization sequence (NSL) 形成非活化態的複合物 (Moynagh, 2005; Perkins, 2007)。已知活化NF-κB的路徑可分為canonical及non-canonical，當細胞受到前發炎細胞激素(包括TNF-α、IL-1) 的刺激或暴露在細菌產物 (lipopolysaccharide, LPS) 下會迅速活化canonical路徑，IKK複合物會快速的將IκBα的Ser32及Ser36磷酸化，促進IκBα接上泛素 (ubiquitin) 並透過26S溶酶體 (proteosome) 降解 (Hayden and Ghosh, 2004)。IKK複合物包含了三個次單元IKKα、IKKβ及IKKγ (NF-κB essential modulator，NEMO)。IKKα與IKKβ皆參與canonical路徑，但研究指出在canonical路徑中IKKβ為主要的IκB kinase (Bonizzi and Karin, 2004)；IKKγ為不具激酶活性的調節次單元，對於IKKα/IKKβ的磷酸化相當重要 (Rothwarf et al., 1998)。透過CD40、lymphotoxin-β 接受器或

TNF家族中的B-cell-activation factor等的刺激可活化non-canonical路徑。在non-canonical路徑中最常見的為p52-RelB異質二聚體，它主要受到IKKα同質二聚體的調控 (Bonizzi and Karin, 2004)。活化後的NF-κB能進入細胞核結合至基因啟動子上的κB位置，並與其輔因子 (cofactor) 產生交互作用藉以調控轉錄作用。NF-κB參與調控轉錄作用上還有其他調節者協助調控，透過轉譯後磷酸化與乙醯基化 (acetylation) 修飾NF-κB的次單元對於其促進基因轉錄具有加強作用 (Chen and Greene, 2004)。例如：p65次單元中的絲胺酸可被磷酸化，而磷酸化的p65與其輔因子產生交互作用進一步被乙醯基化後便具有最高的轉錄活性 (Chen and Greene, 2003)。其中，cAMP respose element binding protein (CREB) binding protein (CBP)/p300便具有factor acetyltransferase (FAT) 的活性，可將轉錄因子乙醯基化 (Vo and Goodman, 2001)。有文獻指出干擾NF-κB與CBP之間的交互作用可明顯減少與NF-κB相關之轉錄作用 (Parker et al., 1999)，例如：具有抗發炎作用的tranilast便是透過減少血管內皮細胞中CBP的蛋白質表現而影響NF-κB相關的轉錄作用，減少TNF-α誘發細胞表面ICAM-1、VCAM-1及E-selectin表現量 (Spiecker et al., 2002)；另外，過度表現p65與CBP可加強轉殖到COS-7細胞內E-selectin或VCAM-1啟動子的報導基因表現，但如果同時使12S E1A過度表現 (12S E1A本身會與CBP/p300結合) 則會減弱報導基因的表現 (Gerritsen et al., 1997)。

- IKK/NF-κB 與動脈粥狀硬化

NF-κB 參與調控免疫反應相關的蛋白質 (IL-2 receptor、tissue factor 及 platelet-activating factor receptor 等)、黏著分子 (ELAM-1、VCAM-1 及 ICAM-1 等)、細胞激素 (TNF-α、IL-1β、IL-2、IL-6、IL-8 及 IL-12

等)、生長因子 (granulocyte colony-stimulating factor，G-CSF) 和趨化細胞激素等的基因表現，這些蛋白質產物與許多發炎反應之疾病有關，其中包括動脈粥狀硬化。NF-κB 不僅會受到發炎細胞激素的刺激而活化，活化後又會誘發這些細胞激素的表現，因此更加強了 NF-κB 的活化作用 (Sun and Andersson, 2002)。研究指出當給與大鼠高脂飲食會明顯增加其內皮細胞及動脈平滑肌細胞 NF-κB 的活化並造成動脈粥狀硬化的產生 (Du et al., 2009)。而給予 NEMO/IKKγ 基因剔除的 ApoE$^{-/-}$小鼠 (NEMO^{EC-KO}/ApoE$^{-/-}$) 與 ApoE$^{-/-}$小鼠高膽固醇飲食後發現，在 NEMO^{EC-KO}/ApoE$^{-/-}$小鼠明顯減少動脈粥狀硬化斑塊的形成。此外，在 dominant-negative IκBα (DNIκBα) 基因轉殖的 ApoE$^{-/-}$小鼠 (其血管內皮所表現的 IκBα 無法被降解) 實驗中發現注射 LPS 後會誘發 ApoE$^{-/-}$小鼠主動脈的 VCAM-1 表現，但在 DNIκBα 基因轉殖的 ApoE$^{-/-}$小鼠卻不會表現，且給予高膽固醇飲食後 DNIκBα 基因轉殖的 ApoE$^{-/-}$小鼠其動脈粥狀硬化斑塊的形成亦明顯比 ApoE$^{-/-}$小鼠少，而這些結果顯示抑制內皮細胞 NF-κB 的活化與降低動脈粥狀硬化損傷有關 (Gareus et al., 2008)。

2. cAMP/protein kinase A (PKA)/CREB

生物體因應個體需求或環境因素會刺激荷爾蒙等物質的分泌，而這些物質必須由細胞膜表面的接受器辨認後，利用二級訊息傳遞分子以進行一連串的訊息傳遞作用。當細胞膜表面的 G protein-coupled receptor 受到刺激活化後會進一步去活化 adenylyl cyclase (AC)，造成 ATP 水解產生 cAMP。cAMP 在細胞中為重要的二級訊息傳遞分子，而 cAMP-dependent protein kinase (PKA) 的活化被認為與增加胞內 cAMP 濃度有關。PKA 為異質四聚

體的酵素複合物，由兩個催化次單元與兩個調控次單元所組成，調控次單元對催化次單元具有抑制作用。在調控次單元的 C 端有 cAMP binding domain，一旦 cAMP 與調控次單元結合後會造成 PKA 酵素複合物的構型改變使得催化次單元與調控次單元分離，活化型的催化次單元便可藉由磷酸化相關的細胞質內或細胞核內蛋白質影響許多生理作用 (Taylor et al., 1990)。

轉錄因子 cAMP-responsive element-binding protein (CREB) 的磷酸化與 PKA 的活化有關。CREB 包含一個 kinase-inducible activation domain (KID)，而其蛋白質上的 Ser133 可被 PKA 磷酸化。當 CREB 磷酸化後會結合至基因啟動子上的 cAMP responsive elements (CREs) 並與輔因子 CBP/p300 產生交互作用藉以調控下游基因表現 (Michael et al., 2000; Ziff, 1990)。研究指出阻斷 CREB 與 CBP 間的交互作用可明顯降低 CREB 相關的轉錄作用 (Parker et al., 1999)。

- cAMP/PKA/CREB 與動脈粥狀硬化

  已知動脈粥狀硬化為慢性發炎疾病，而轉錄因子 NF-κB 在發炎反應中扮演重要的角色。許多研究顯示增加胞內 cAMP 或活化 PKA 可抑制由 NF-κB 所調控的基因轉錄作用，但此抑制作用並非透過干擾 NF-κB 進入細胞核內，而是藉由活化的 CREB 與 p65 彼此互相競爭 CBP (Ollivier et al., 1996; Parry and Mackman, 1997)。在將報導基因轉殖到 HUVECs 的研究中發現過度表現 CBP 可明顯降低 forskolin 對 NF-κB 轉錄作用的抑制效果，而過度表現 CREB 則可加強 forskolin 抑制 NF-κB 所調控的轉錄作用 (Parry and Mackman, 1997)。在 Jurkat T-lymphocytes 中無論是直接處理 PKA 活化劑 (forskolin、dibutyryl cAMP 與

8-bromo-cAMP) 或藉由過度表現 PKA 的催化次單元皆能抑制 NF-κB 的轉錄活性 (Takahashi et al., 2002)。此外，細胞激素在動脈粥狀硬化發展的過程中亦相當重要，有研究指出 forskolin 與 dibutyryl cAMP (cAMP 相似物) 具有抑制 LPS 誘發人類單核球細胞產生 TNF-α 的效果 (Shames et al., 2001)。而 HUVECs 預處理 forskolin 可顯著抑制 TNF-α 誘發 E-selectin 與 VCAM-1 的 mRNA 表現；人類單核球細胞 (THP-1) 預處理 dibutyryl cAMP 則可明顯減少 LPS 誘發 TNF-α 的 mRNA 表現 (Ollivier et al., 1996)。除了直接利用 dibutyryl cAMP 處理 THP-1 細胞可抑制其黏附於以 TNF-α 處理的 HUVECs 之外，臨床上應用於抗血小板凝集的藥物 cilostazol 為 Type Ⅲ phosphodiesterase (PDE3) 的抑制劑，亦具有增加胞內 cAMP 的作用，THP-1 細胞在 cilostazol 的處理下也可抑制其對活化的內皮細胞之黏附作用 (Mori et al., 2007)。以上這些研究顯示透過活化 cAMP/PKA/CREB 路徑能抑制 NF-κB 相關的轉錄作用，或許能藉此達到降低動脈粥狀硬化損傷之效果。

研究目的

本實驗室先前研究發現以穿心蓮內酯預處理 HUVECs 可抑制由 TNF-α所誘發的 ICAM-1 蛋白質表現，而 NFκB signaling pathway 在以前的實驗被證實對細胞黏著分子的表現扮演重要角色，因此本實驗利用人類血管內皮細胞(EA.hy926)為模式探討穿心蓮內酯抑制腫瘤壞死因子刺激 ICAM-1 表現的機制是否是透過影響 NF-κB signaling pathway。

第二部分

Effect of andrographolide on tumor necrosis factor-alpha-induced intercellular adhesion molecule-1 expression in EA.hy926 cells

Introduction

Andrographis paniculata (Burm.f.) Nees (Acanthaceae), a well-known traditional medicinal plant in India, Thailand, and China, has attracted great attention recently because of its clinical application potential. There are diterpene lactones, flavonoids and polyphenols in *A. paniculata*. Andrographolide is a major bioactive diterpene lactone in *A. paniculata*, which is concentrated in leaves. Many studies have shown that andrographolide possesses anti-inflammatory (Abu-Ghefreh et al., 2009; Bao et al., 2009), anti-tumor (Jiang et al., 2007; Zhao et al., 2008), anti-viral (Chen et al., 2009), anti-oxdative (Akowuah et al., 2008), anti-hyperglycemic (Yu et al., 2003), and hepatoprotective (Trivedi et al., 2007) properties. The anti-inflammatory property of andrographolide has been extensively studied both *in vivo* and *in vitro*. Andrographolide attenuated ovalbumin-induced airway inflammation in BALB/c mice through reduced expression of cytokines and chemokines (Bao et al., 2009). In human neutrophils, andrographolide prevented reactive oxygen species (ROS) production, and decreased macrophage adhesion molecule-1 (Mac-1) expression induced by N-formyl-methionyl-leucyl-phenylalanine (fMLP). This leads to inhibition of neutrophil adhesion and transmigration (Shen et al., 2002).

Atherosclerosis is a chronic inflammatory response. Increasing plasma low-density lipoprotein (LDL) was considered an important risk factor, especially. Expression of pro-inflammatory cytokines and adhesion molecules was increased by the activated endothelial cells, which was stimulated by oxidized-LDL

(ox-LDL) or injury on vessel wall. Leukocytes recruitment and ox-LDL uptake stimulate growth of plaque, and further formation of fatty lesions. Reinforcement of inflammation may lead to local proteolysis, plaque rupture, and thrombus formation, which lead to ischemia and infarction (Hansson, 2005, 2009). Cytokines and adhesion molecules both play important roles in leukocyte recruitment. During atherosclerotic progression, adhesion molecules were involved in adhesion and transendothelial migration of leukocytes (Galkina and Ley, 2007). Kaufmann et al. (2007) demonstrated that adhesion molecule expression at atherosclerotic plaques by immunohistochemistry. Cytokines including IL-1 and TNF-α induce the expression of E-selectin, VACM-1, and ICAM-1 through NF-κB activation in human endothelial cells (Lin et al., 2007; Zakeri et al., 2000; Zhou et al., 2007).

ICAM-1, a transmembrane glycoprotein, is regarded as an inflammatory indicator. In comparison with the other transcription factor (e.g., AP-1 and STAT) binding sites of ICAM-1 promoter, NF-κB binding site plays a critical role in TNF-α-induced ICAM-1 expression (Oh et al., 2010). NF-κB is involved in the regulation of gene expression of inflammatory and immune responses. The NF-κB family comprises five members, and they are RelA (p65), RelB, c-Rel, p50/p105 (NF-κB1), and p52/p100 (NF-κB2). NF-κB subunits are dimerized and retained in cytoplasm with inhibitory protein, IκB. Activation of IKK complex causes the phosphorylation of IκB family and subsequent degradation by 26S proteasome. Free NF-κB complex then translocates to the nucleus and binds to the κB element of target genes (Hayden and Ghosh, 2004). In nucleus, transcription activity of

NF-κB is modulated by cofactors, such as CBP (CREB binding protein) /p300 (Chen and Greene, 2003, 2004).

Increasing intracellular cAMP leads to activation of protein kinase A and induces the expression of many genes through regulation of transcription factors, such as cAMP respose element binding protein (CREB). Phospho-CREB allows recruitment of its cofactors, CREB binding protein (CBP)/p300, then binds to cAMP respose element (CRE) of target genes and turns on gene transcription (Michael et al., 2000; Ziff, 1990). Interference with the interaction between CBP and transcription factors can alter relevant gene transcription. For example, tranilast reduced CBP expression in vascular endothelial cells which led to inhibition of TNF-α-induced ICAM-1, VCAM-1, and E-selectin expressions (Spiecker et al., 2002). The expressions of ICAM-1, VCAM-1, and E-selectin were NF-κB-dependent (Lin et al., 2007; Zakeri et al., 2000; Zhou et al., 2007). NF-κB-mediated gene expression was attenuated by CREB activation and this was due to the competitive binding of CBP between CREB and p65 (Parry and Mackman, 1997). Treatment of HUVECs with forskolin reduced NF-κB-dependent gene transcription. The suppression effect of forskolin was enhanced by CREB overexpression but reversed by CBP overexpression (Parry and Mackman, 1997). Many studies have shown that increase in intracellular cAMP level by PKA activators, including forskolin and cAMP analogues, reduced TNF-α production or E-selectin, VCAM -1, and ICAM-1 mRNA levels induced by LPS, TNF-α, or IL-1β in coronary artery tissue and coronary smooth muscle cells of pig, human monocytes, HUVECs, or brain endothelial cells, respectively (Balyasnikova et al., 2000; Newman et al., 1998; Ollivier et al., 1996; Shames et

al., 2001).

In the present study, we determined the effect of andrographolide on ICAM-1 expression induced by TNF-α in endothelial cells, EA.hy926. In addition, we investigated the involvement of NF-κB and CREB in TNF-α-induced ICAM-1 expression by andrographolide. The results of this study will provide a mechanism exploring the anti-inflammatory effect of andrographolide.

Materials and Methods

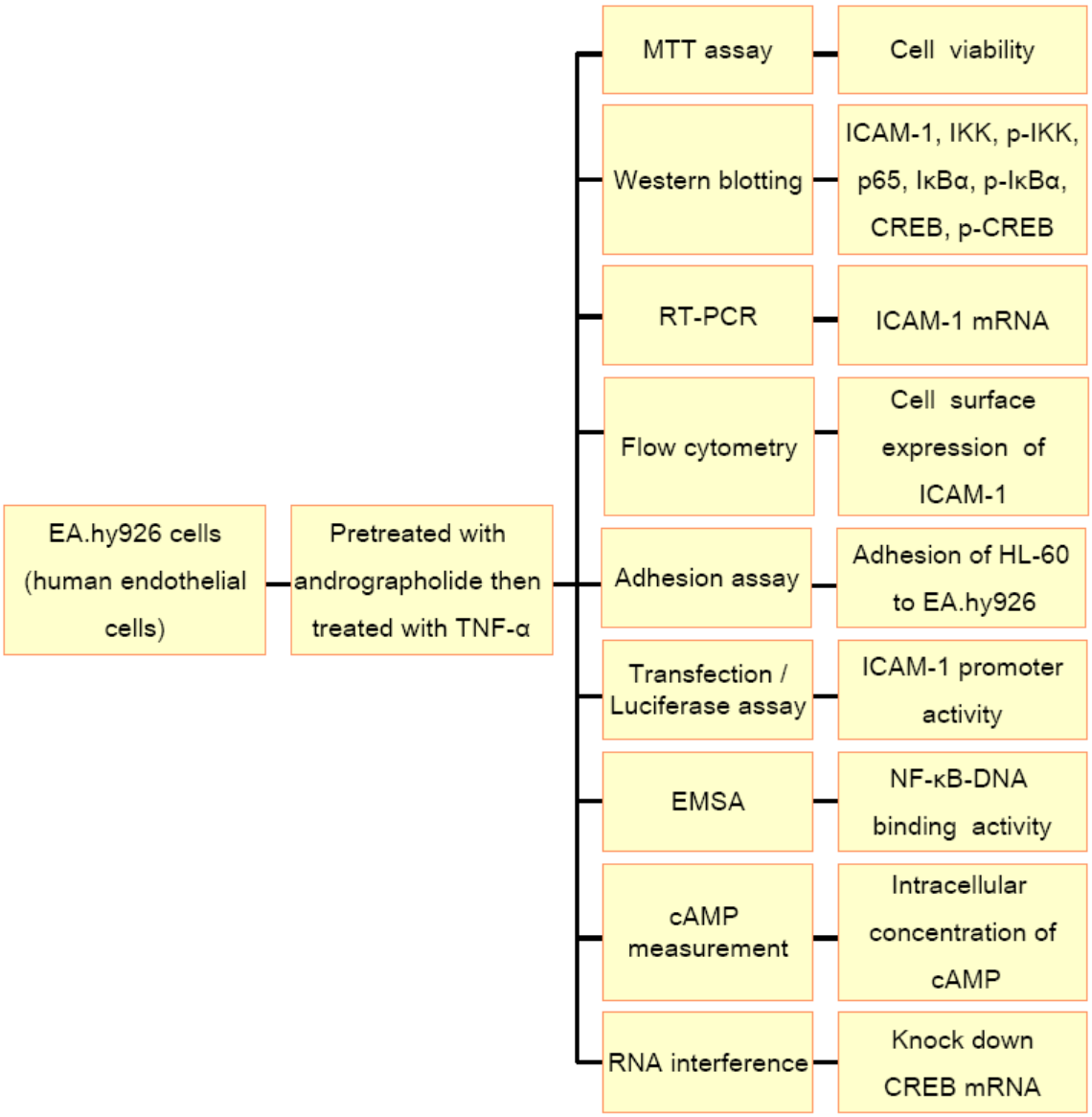

Reagents

Cell culture medium Dulbecco's modified Eagles medium (DMEM), RPMI-1640, RPMI-1640 (without phenol red), OPTI-MEM, 0.25% trypsin-EDTA, and penicillin/streptomycin were from GIBCO-BRL (Grand Island, NY); HBSS and fetal bovine serum (FBS) were from HyClone (Logan, UT); andrographolide (AP) was from Calbiochem (Darmstadt, Germany); human tumor necrosis factor-alpha (TNF-α), sodium bicarbonate, and 3-(4,5-dimethylthiazol-2-yl)-2,5-diphenyltetrazolium bromide (MTT) were from Sigma (St. Louis, MO); *bis*-Carboxyethyl-carboxyfluorescein acetoxymethyl ester (BCECF-AM) was from Molecular Probes (Eugene, OR); anti-actin, anti-ICAM-1, anti-CREB, anti-phospho-CREB (Ser 133), anti-phospho-IκBα (Ser32/36) and anti-phospho IKKα (Ser180)/ IKKβ (Ser181) antibodies were from Cell Signaling Technology (Boston, MA); anti- IκBα and anti-IKKα/ β antibodies were from Santa Cruz Biotechnology (Santa Cruz, CA); anti-p65 antibody was from BD Bioscience (San Jose, CA); fluorescein isothiocyanate-conjugated mouse anti-human ICAM-1 antibody was from Serotec Company (Kidlington, Oxford, UK); polyvinylidene difluoride membrane was from Millipore (Billerica, MA); TRIzol reagent was from Invitrogen (Carlsbad, CA); ethanol, isopropyl alcohol, and chloroform were from Merck (Darmstadt, Germany); Hybond-N^+ nylon transfer membrane was from GE Healthcare (Buckinghamshire, UK); and the transfection reagent Dharmafect 1 was from Dharmacon (Lafayette, CO). The oligonucleotide primers for electrophoretic mobility shift assay (EMSA), the biotin-labeled and unlabeled double-stranded NF-*κ*B consensus oligonucleotide, and a mutant double-stranded NF-*κ*B oligonucleotide were synthesized by MDBio

Inc. (Taipei, Taiwan), predesigned small interfering RNA (siRNA) against human CREB, and non-targeting pool were purchased from Dharmacon Research, Inc (Lafayette, CO).

Cell cultures

The human endothelial cell line EA.hy926 was cultured in DMEM supplemented with 3.7 g/L $NaHCO_3$, 10% FBS, 100 U penicillin/mL, and 100 μg streptomycin/mL at 37°C in a 5% CO_2 humidified incubator. The human leukemia promyelocytic cells (HL-60) were purchased from Bioresources Collection and Research Center (BCRC, HsinChu, Taiwan).The HL-60 cells were cultured in T-75 tissue culture flasks in RPMI 1640 medium supplemented with 10% fetal bovine serum, 100000 U/L penicillin, and 100 mg/L streptomycin. Cells were incubated at 37℃ in 5% CO_2 humidified incubator.

Cell viability assay

Cell viability was assessed by the MTT assay. The MTT assay measures the ability of viable cells to reduce a yellow 3-(4,5-dimethylthiazol-2-yl)-2,5-diphenyltetrazolium bromide to a purple formazan by mitochondrial succinate dehydrogenase. EA.hy926 cells were grown to 70-80% confluence and were then treated with different concentrations of andrographolide (0-20 μM) for 16 h followed by incubation with TNF-α (1 ng/mL) for another 6 h. Finally, the DMEM medium was removed, and the cells were washed with PBS. The cells were then incubated with MTT (0.5 mg/mL) in DMEM medium at 37°C for an additional 3 h. The medium was removed, and isopropanol was added to dissolve the formazan.

After centrifugation at 20000×*g* for 5 min, the supernatant of each sample was transferred to 96-well plates, and absorbance was read at 570 nm in an ELISA reader. The absorbance in cultures treated with 0.1% DMSO was regarded as 100% cell viability.

Nuclear extracts preparation

After each experiment, cells were washed twice with cold PBS and were then scraped from the dishes with 1000 μL of PBS. Cell homogenates were centrifuged at 2000×*g* for 5 min. The supernatant was discarded, and the cell pellet was allowed to swell on ice for 15 min after the addition of 200 μL of hypotonic buffer containing 10 mM HEPES, 1 mM $MgCl_2$, 1 mM EDTA, 10 mM KCl, 0.5 mM DTT, 0.5% Nonidet P-40, 4 μg/mL leupeptin, 20 μg/mL aprotinin, and 0.2 mM PMSF. After centrifugation at 7000x*g* for 15 min, pellets containing crude nuclei were resuspended in 50 μL of hypertonic buffer containing 10 mM HEPES, 400 mM KCl, 1 mM $MgCl_2$, 0.25 mM EDTA, 0.5 mM DTT, 4 μg/mL leupeptin, 20 μg/mL aprotinin, 0.2 mM PMSF, and 10% glycerol at 4^{o}C for 30 min. The samples were then centrifuged at 20000×*g* for 15 min. The supernatant containing the nuclear proteins was collected and stored at -80^{o}C until the Western blotting and electrophoretic mobility shift assays.

Western blotting analysis

After each experiment, cells were washed twice with cold PBS and were harvested in 150 μL lysis buffer (10 mM Tris-HCl, pH 8, 0.1% Triton X-100, 320 mM sucrose, 5 mM EDTA, 1 mM PMSF, 1 mg/L leupeptin, 1 mg/L aprotinin, and

2 mM dithiothreitol). Cell homogenates were centrifuged at 14000×*g* for 20 min at 4°C. The resulting supernatant was used as a cellular protein for Western blot analysis. The preparation of nuclear extracts was described above. The total protein was analyzed by use of the Coomassie Plus protein assay reagent kit (Pierce Biotechnology Inc., Rockford, IL). Equal amounts of cellular proteins were electrophoresed in an SDS-polyacrylamide gel, and proteins were then transferred to polyvinylidene fluoride membranes (Millipore Corporation, Bedford, MA). Nonspecific binding sites on the membranes were blocked with 5% nonfat milk in 15 mM Tris/150 mM NaCl buffer (pH 7.4) at room temperature for 2 h. Membranes were probed with rabbit anti-human anti-actin, anti-ICAM-1, anti-CREB, anti-phospho-CREB (Ser 133), anti-phospho-IκBα (Ser32/36) and anti-phospho IKKα (Ser180)/ IKKβ (Ser181), anti- IκBα and anti-IKKα/ β, and anti-p65 antibodies. The membranes were then probed with the secondary antibody labeled with horseradish peroxidase. The bands were visualized by using an enhanced chemiluminescence kit (PerkinElmer Life Science, Boston, MA) and were scanned by a luminescent image analyzer (FUJIFILM LAS-4000, Japan). The bands were quantitated with an ImageGauge (FUJIFLM).

RNA isolation and reverse transcription-polymerase chain reaction (RT-PCR)

Total RNA of EA.hy926 cells was extracted by using Trizol reagent. After treatment, cells were washed twice with cold PBS and scraped with 500 μL of Trizol reagent. Cell samples were mixed with 100 μL of chloroform and centrifuged at 11000×*g* for 15 min. The supernatant was collected and mixed with

250 μL of isopropyl alcohol. After centrifugation at 12000×*g* for 20 min, the supernatant was discarded and the cell pellet was stored in 70% ethanol or dissolved in deionized water for quantification. We used 0.2 μg total RNA for the synthesis of first-strand cDNA by using Moloney murine leukemia virus reverse transcriptase (Promega Company, Madison, WI) in a 20-μL final volume containing 250 ng oligo-dT and 40 U RNase inhibitor. PCR was carried out in a thermocycler in a 50-μL reaction volume containing 20 μL of cDNA, BioTaq PCR buffer, 50 μmol of each deoxyribonucleotide triphosphate, 1.25 mmol/L $MgCl_2$, and 1 U of BioTaq DNA polymerase (BioLine). Oligonucleotide primers of ICAM-1 (forward: 5'-TGAAGGCCACCCCAGAGGACAAC-3'; reverse: 5'-CCCATTATGACTGCGGCTGCTGCTACC-3') and glyceraldehyde 3-phosphate dehydrogenase (forward: 5'-CCATCACCATCTTCCAGGAG-3'; reverse: 5'-CCTGCTTCACCACCTTCTTG-3') were designed on the basis of published sequences (Meagher et al., 1994). Amplification of ICAM-1 and GAPDH was performed by heating samples to 95°C for 5 min and then immediately cycling 32 times through a 1-min denaturing step at 94°C, a 1-min annealing step at 56°C, and a 1-min elongation step at 72°C. The glyceraldehyde 3-phosphate dehydrogenase cDNA level was used as the internal standard. PCR products were resolved in a 1%-agarose gel and were scanned by using a Digital Image Analyzer (Alpha Innotech) and quantitated with an ImageGauge.

ICAM-1 expression on cell surfaces

The expression of ICAM-1 on plasma membranes was measured by fluorescence flow cytometry. After experiment, cells were suspended in 0.25%

trypsin and centrifuged at 2000×*g* for 5 min. The supernatant was discarded and cells were reacted with fluorescein isothiocyanate–conjugated mouse anti-human ICAM-1 antibody at 4℃ for 45 min in the dark. Cells were washed 3 times with cold PBS and fluorescence was read by use of a Becton Dickinson FACSCalibur (BD Biosciences, San Jose, CA).

Monocyte adhesion assay

EA.hy926 cells in 12-well plates were allowed to grow to 80% confluence and were then pretreated with andrographolide for 16 h followed by incubation with 1 ng/mL TNF-α for another 6 h. The human monocytic HL-60 cells cultured in RPMI 1640 medium with 10% FBS were labeled with 1 μM 2,7-bis(2-carboxyethyl)-5(6)-carboxyfluorescein acetoxymethylester (BCECF-AM). At the end of andrographolide and TNF-α treatment, a total of 1×10^6 BCECF-AM-labeled HL-60 cells were added to each well, and the cells were co-incubated with EA.hy926 at 37^{o}C for 30 min. The wells were washed and filled with cell culture medium, and the plates were sealed, inverted, and centrifuged at 100×*g* for 5 min to remove nonadherent HL-60 cells. Bound HL-60 cells were lysed in a 1% SDS solution, and the fluorescence intensity was determined in a fluoroscan ELISA plate reader (FLX800, Bio-Tek, Winooski, VT) with an excitation wavelength of 480 nm and an emission wavelength of 520 nm. A control study showed that fluorescence is a linear function of HL-60 cells in the range of 3000–80000 cells/well. The results are reported on the basis of the standard curve obtained.

Plasmid, transfection and luciferase assays

The ICAM-1 promoter-luciferase construct (pIC339, -339 to 0) was a gift from Dr. P. T. van der Saag (Hubrecht Laboratory, Utrecht, The Netherlands). pIC339 contains NF-κB (-187/-178), AP-1 (-284/-279), AP-2 (-48/-41), and Sp1 (-59/-53, -206/-201) biding sites (van de Stolpe et al., 1994). EA.hy926 cells were transiently transfected for 4 h with 0.1 μg of pIC339 plasmid and 0.1 μg of β-galactosidase plasmid by using 1 μL of nanofectin (PAA, Pasching, Austria) in OPTI-MEM medium. After transfection, cells were changed to DMEM medium and treated with AP for 16 h before being challenged with TNF-α for additional 5 h. Cells were then washed twice with cold PBS, scraped with lysis buffer (Promega, Madison, WI), and centrifuged at 14000×*g* for 3 min. The supernatant was collected for the measurement of luciferase and β-galactosidase activities by using Luciferase Assay Kit (Promega, Madison, WI) according to the manufacturer's instructions. The luciferase activity of each sample was corrected on the basis of β-galactosidase activity, which was measured at 420 nm with O-nitrophenyl-b-D-galactopyranoside as a substrate. The value for cells treated with 0.1% DMSO (control) was set at 1.

Electrophoretic mobility shift assay (EMSA)

EMSA was performed according to our previous study (Cheng et al., 2004). The LightShift Chemiluminescent EMSA Kit (Pierce Chemical Company, Rockford, IL) and synthetic biotin-labeled double-stranded κB consensus oligonucleotides (forward: 5′-AGTTGAGGGGACTTTCCCAGGC-3′; reverse: 5′-GCCTGGGAAAGTCCCCTCAACT-3′) were used to measure NF-κB nuclear

protein-DNA binding activity. Ten micrograms of nuclear extract, poly (dI-dC), and biotin-labeled double-stranded NF-κB oligonucleotides were mixed with the binding buffer (Chemiluminescent Nucleic Acid Detection Module, Thermo, Rockford, IL) to a final volume of 20 μL, and the mixture was incubated at 27℃ for 30 min. Unlabeled double-stranded NF-κB oligonucleotides and a mutant double-stranded oligonucleotides (5′-AGTTGAGGCGACTTTCCCAGGC-3′) were used to confirm the protein-binding specificity. The nuclear protein-DNA complex was separated by electrophoresis on a 6% TBE-polyacrylamide gel and was then transferred to a Hybond-N+ nylon membrane. The membranes were cross-linked by UV light for 10 min and were then treated with 20 μL of streptavidin-horseradish peroxidase for 20 min, and the nuclear protein-DNA bands were developed with a Chemiluminescent Substrate (Thermo, Rockford, IL). The bands were scanned by a luminescent image analyzer (FUJIFILM LAS-4000, Japan).

Measurement of intracellular cAMP concentrations

After treatment, cells were washed twice with cold PBS and lysed and scraped into 200 μL of 0.1 N HCl. Cell homogenates were centrifuged at 1000×*g* for 10 min. The resulting supernatant was collected for the measurements of cAMP and protein. Intracellular cAMP concentrations were measured by using the cAMP EIA kit (Cayman Chemical Company, Ann Arbor, MI). For cAMP measurements, cell extracts, cAMP AChE tracer, and cAMP antiserum were coincubated in the 96-well plate at 4^{o}C for 18 h. After then, wells were washed five times with washing buffer, addition of 200 μL of Ellman's Reagent and incubated for 120

min. Read the plate at a wavelength of 415 nm. The protein content was determined by using the Coomassie Plus protein assay reagent kit. cAMP concentrations in the control are expressed as 100%, and the concentrations in the other groups were calculated in comparison with the control.

RNA interference by small interfering RNA of CREB

Predesigned small interfering RNA (siRNA) against human CREB and non-targeting control-pool siRNA were purchased from Dharmacon Inc. (Lafayette, Colorado). EA.hy926 cells were cultured and allowed to grow to 80% confluence. EA.hy926 cells were transfected with CREB siRNA SMARTpool by using DharmaFECT1 transfection reagent (Thermo) according to the manufacturer's instructions. The 4 siRNAs against the human CREB gene are (1) GAGAGAGGUCCGUCUAAUG, (2) UAGUACAGCUGCCCAAUGG, (3) CAACUCCAAUUUACCAAAC, and (4) GCCCAGCCAUCAGUUAUUC. A non-targeting control-pool siRNA was also tested. Non-targeting control-pool was as negative control (NTC). After 8 h of transfection, cells were treated with AP for 16 h before incubation with TNF-α for another 6 h. Cell samples were collected for Western blotting analysis.

Statistical analysis

Data were analyzed by using analysis of variance (SAS Institute, Cary, NC). The significance of the difference among mean values was determined by one-way analysis of variance followed by the Tukey's test. *P* values < 0.05 were taken to be statistically significant.

Results

Cell viability

The MTT assay was used to evaluate whether the concentrations of andrographolide or andrographolide and TNF-α used caused cell damage in EA.hy926 cells. As shown in panels A and B of Figure 1, the cell viability of EA.hy926 cells was more than 85% up to an andrographolide concentration of 10 μM in the presence or absence of 1 ng/mL TNF-α, which was used to induce the expression of ICAM-1. The highest concentration of andrographolide used in this study was 10 μM, and thus, the effects of andrographolide observed below were not due to its cytotoxicity.

Andrographolide inhibits TNF-α-induced ICAM-1 expression in EA.hy926 cells

TNF-α (1 ng/mL) significantly induced ICAM-1 expression in EA.hy926 cells ($p < 0.05$) and the induction pattern was time-dependent (Figure 2). EA.hy926 cells were pretreated with 10 μM andrographolide for the indicated times before being exposed to 1 ng/mL TNF-α for 6 h. The protein expression of ICAM-1 was significantly suppressed after pretreatment for 4 h compared with that treated with TNF-α alone, and the inhibition was sustained with pretreatment for up to 24 h (Figure 3). To determine whether the TNF-α-induced protein and mRNA expression of ICAM-1 were dose-dependently affected by andrographolide, concentrations of andrographolide ranging from 0 to 10 μM were studied. As shown in panels A and B of Figure 4, the inhibition of TNF-α-induced protein and mRNA expression of ICAM-1 by andrographolide was in a dose-dependent

manner. A significantly inhibitory effect of andrographolide on ICAM-1 protein expression was observed at concentrations greater than 5 μM, and a significantly inhibitory effect on ICAM-1 mRNA expression was observed at concentrations greater than 10 μM. The expression of ICAM-1 on cell surfaces was determined by flow cytometry. Cells pretreated with 5 and 10 μM andrographolide had significantly lower ICAM-1 expression on cell surfaces compared with those treated with TNF-α alone (Figure 5).

Andrographolide inhibits TNF-α-induced HL-60 cell adhesion

We next determined whether andrographolide pretreatment could inhibit HL-60 cell adhesion. As shown in Figure 6, TNF-α significantly increased HL-60 cell adhesion. However, andrographolide pretreatment inhibited HL-60 cell adhesion in a dose-dependent manner, and a significant inhibitory effect was found at 10 μM.

Andrographolide inhibits TNF-α-induced ICAM-1 luciferase reporter activity

To investigate the role of andrographolide in TNF-α-induced ICAM-1 gene transcription, promoter activity assays were performed using a human ICAM-1 promoter-luciferase construct, pIC339 (-339 to 0). TNF-α-induced ICAM-1 promoter activation was inhibited by 5 and 10 μM andrographolide (Figure 7). This result suggests that andrographolide has an inhibitory effect on TNF-α-mediated ICAM-1 promoter activation.

Andrographolide inhibits TNF-α-induced activation of NF-κB

Several putative recognition sequences for a variety of transcriptional activators, including AP-1, retinoic acid-response element (RARE), C/EBP, NF-κB, Ets-1, interferon-stimulated response element (IRE), Sp1, and AP-2 were present in the human proximal ICAM-1 promoter-enhancer region (-346 to -24) (Huang and Chen, 2005). We determined the role of NF-κB in the inhibition of ICAM-1 gene activation by andrographolide. It was reported that NF-κB was activated by IKKα/β (Sakurai et al., 2003). As shown in Figure 8, TNF-α induced both IKKα and IKKβ phosphorylation. The activation of IKKα and IKKβ were significantly attenuated by andrographolide pretreatment. Treatment with TNF-α caused phosphorylation and degradation of IκBα (at 5 min and 15 min, respectively) in EA.hy926 cells. However, the phosphorylation effect was abolished and the degradation effect was attenuated by pretreatment with andrographolide for 16 h (Figure 9). Under basal conditions, NF-κB is sequestered in the cytosol by its inhibitor protein IκBα and remains inactive. After exposure to stimuli, IκBα was phosphorylated and degraded. After then, NF-κB was released and translocated to the nucleus where it binds the response elements of the target genes (Hayden and Ghosh, 2004). To investigate the effect of andrographolide on NF-κB activation, p65 content of nucleus was determiend by Western blotting. Nuclear translocation of p65 was induced by TNF-α, and this effect was attenuated by andrographolide pretreatment (Figure 10). The NF-κB nuclear protein-DNA binding activity was analyzed by EMSA. TNF-α increased NF-κB nuclear protein-DNA complex formation, and pretreatment with andrographolide resulted in the inhibition of NF-κB nuclear protein-DNA complex formation (Figure 11). These results indicate that andrographolide inhibits TNF-α-induced NF-κB activation.

Andrographolide increases intracellular cAMP concentration and induces phosphorylation of CREB in EA.hy926 cells

Many studies have reported that NF-κB-mediated transcription could be attenuated by activation of cAMP/PKA/CREB signaling pathway. This effect was due to the competition for CBP between NF-κB and CREB (Ollivier et al., 1996; Parry and Mackman, 1997; Shames et al., 2001). Our previous study has shown that andrographolide elevated intracellular cAMP and activated CREB in primary hepatocytes (Yang et al., 2010). In order to investigate whether cAMP and CREB were involved in the inhibition of ICAM-1 expression by andrographolide, intracellular cAMP concentration and CREB phosphorylation were analyzed. Intracellular cAMP concentration was significantly increased by treatment with 10 μM andrographolide for 30 min (Figure 12), and the phosphorylation of CREB was significantly increased by treatment with 10 μM andrograpohlide for 0.5 and 2 h (Figure 13).

CREB siRNA shows no effect on andrographolide inhibition of ICAM-1 expression in the presence of TNF-α

To demonstrate whether the competition of CBP by CREB was involved in the inhibition of andrographolide, CREB siRNA was used. After transient transfection with CREB siRNA knocked down CREB expression in EA.hy926 cells. However, CREB siRNA did not affect the inhibition of ICAM-1 expression by andrographolide (Figure 14). These results suggest that CREB is not involved in the suppression of ICAM-1 by andrographolide.

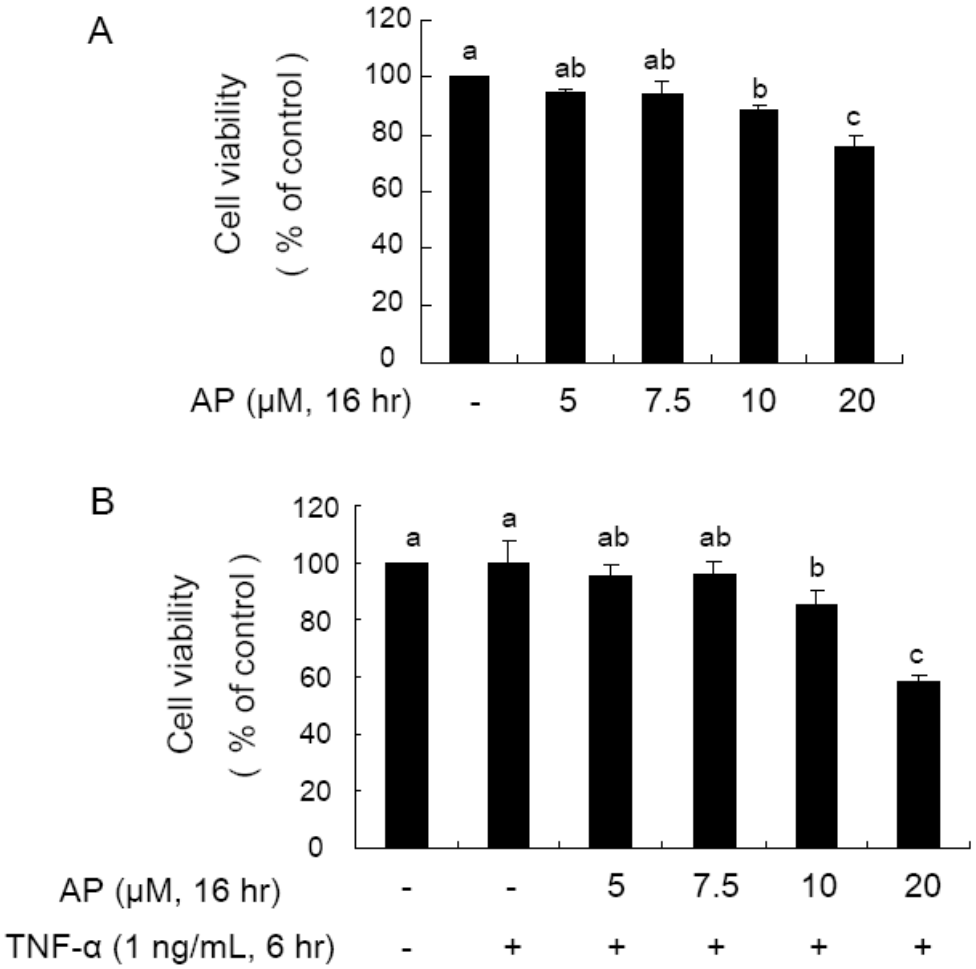

Figure 1. Effect of andrographolide (AP) on the cell viability of EA.hy926 cells in the presence or absence of TNF-α. (A) Cells were treated with 0-20 μM andrographolide for 16 h. (B) Cells were pretreated with 0-20 μM andrographolide for 16 h followed by incubation with 1 ng/mL TNF-α for an additional 6 h. Cell viability was measured by using the MTT assay. Values are means ± SD of three independent experiments. Values not sharing an alphabetic letter are significantly different ($p < 0.05$).

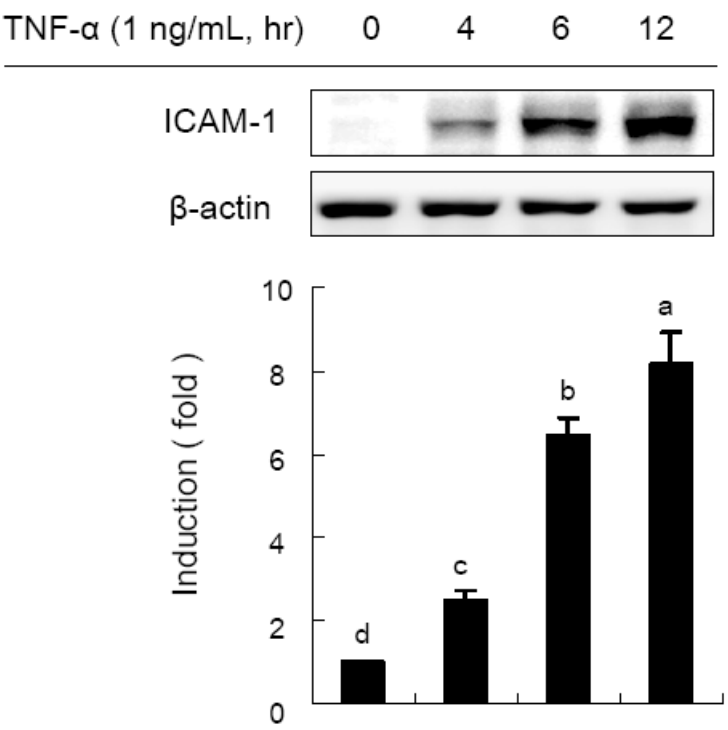

Figure 2. TNF-α induces the expression of ICAM-1 in EA.hy926 cells. Cells were treated with 1 ng/ mL TNF-α for various time periods. Aliquots of total protein (20 μg) were used for Western blot analysis. The levels in control cells were set at 1. Values are means ± SD of three independent experiments. Values not sharing an alphabetic letter are significantly different ($p < 0.05$).

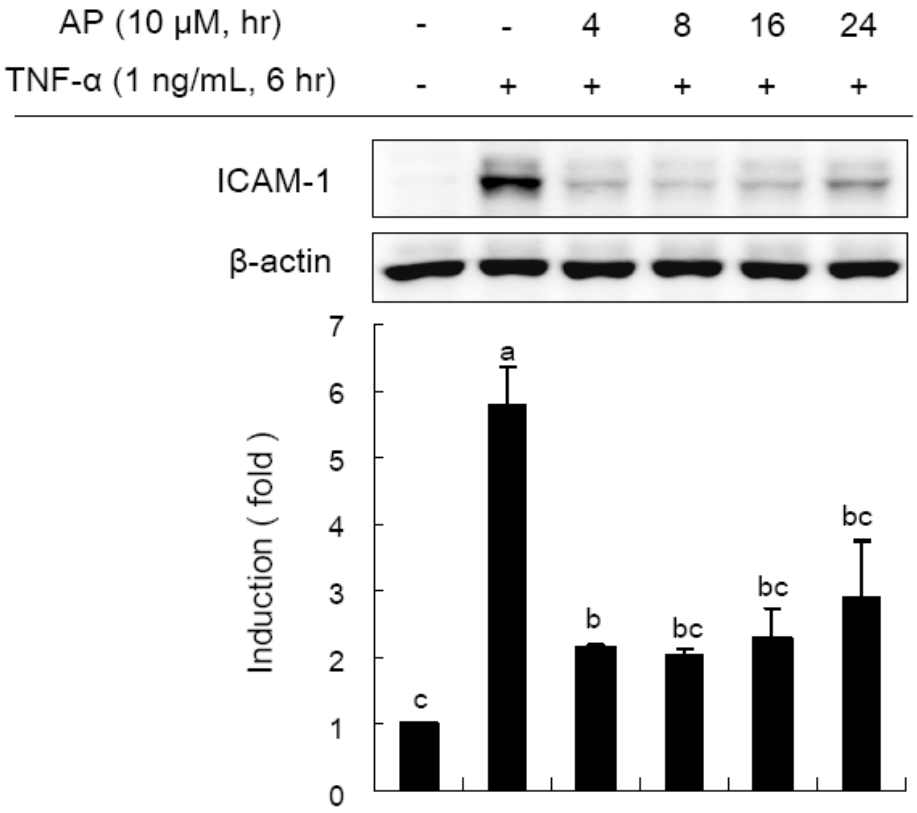

Figure 3. Effect of andrographolide (AP) on TNF-α-induced ICAM-1 protein expression in EA.hy926 cells. Cells were pretreated with 10 μM AP for various time periods followed by incubation with 1 ng/mL TNF-α for an additional 6 h. Aliquots of total protein (20 μg) were used for Western blot analysis. The levels in control cells were set at 1. Values are means ± SD of three independent experiments. Values not sharing an alphabetic letter are significantly different ($p < 0.05$).

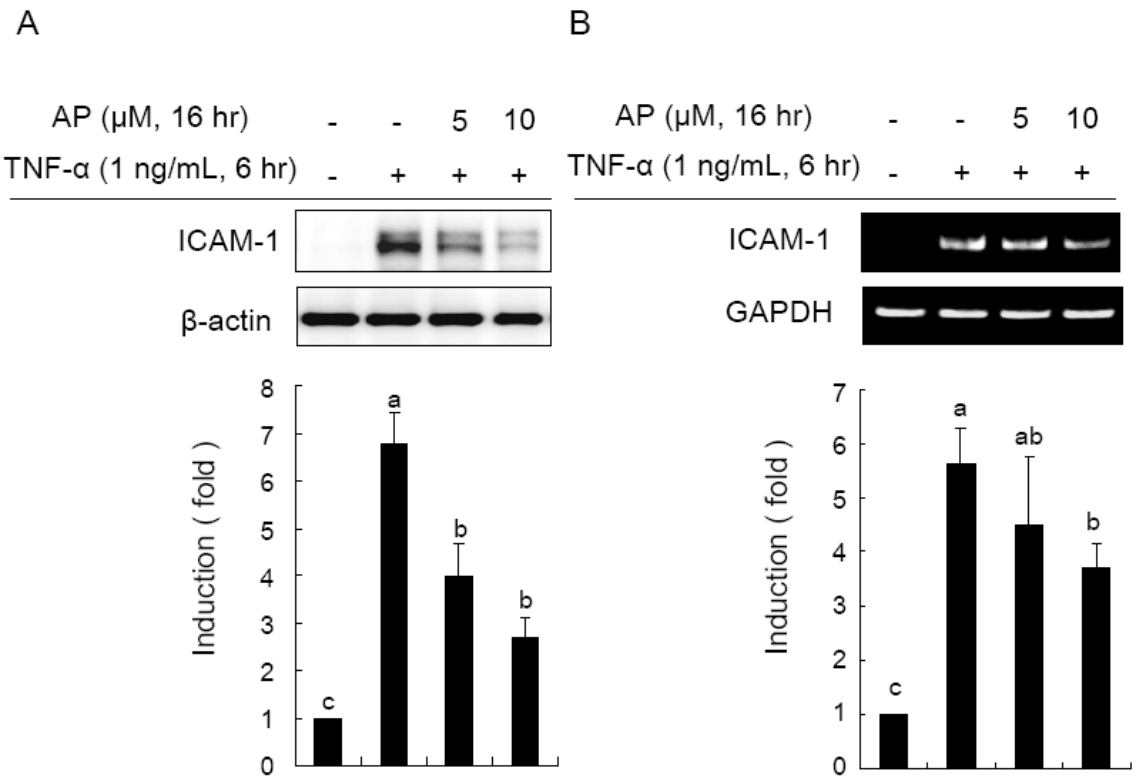

Figure 4. Andrographolide (AP) inhibits ICAM-1 protein and mRNA expression induced by TNF-α in EA.hy926 cells. Cells were pretreated with andrographolide for 16 h followed by incubation with 1 ng/mL TNF-α for an additional 6 h. (A) Aliquots of total protein (20 μg) were used for Western blot analysis. (B) Total RNA was isolated from cells and was subjected to RT-PCR with specific ICAM-1 and GAPDH primers as described in Materials and Methods. The levels in control cells were set at 1. Values are means ± SD of three independent experiments. Values not sharing an alphabetic letter are significantly different ($p < 0.05$).

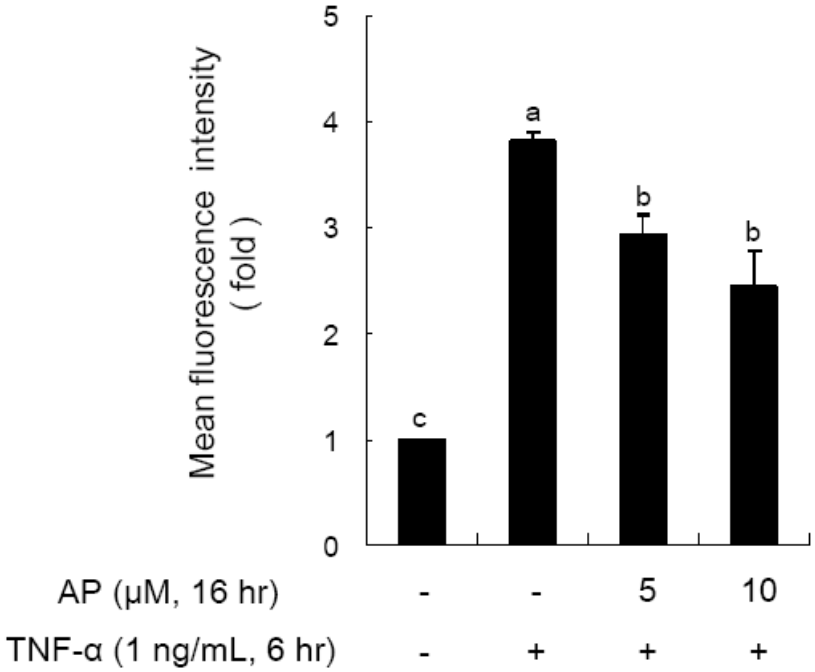

Figure 5. Andrographolide (AP) inhibits TNF-α-induced ICAM-1 protein expression on cell surfaces of EA.hy926 cells. Cells were pretreated with andrographolide for 16 h followed by incubation with 1 ng/mL TNF-α for an additional 6 h. Control cells were maintained in the vehicle before being challenged with TNF-α. The levels in control cells were set at 1. Values are means ± SD of three independent experiments. Values not sharing an alphabetic letter are significantly different ($p < 0.05$).

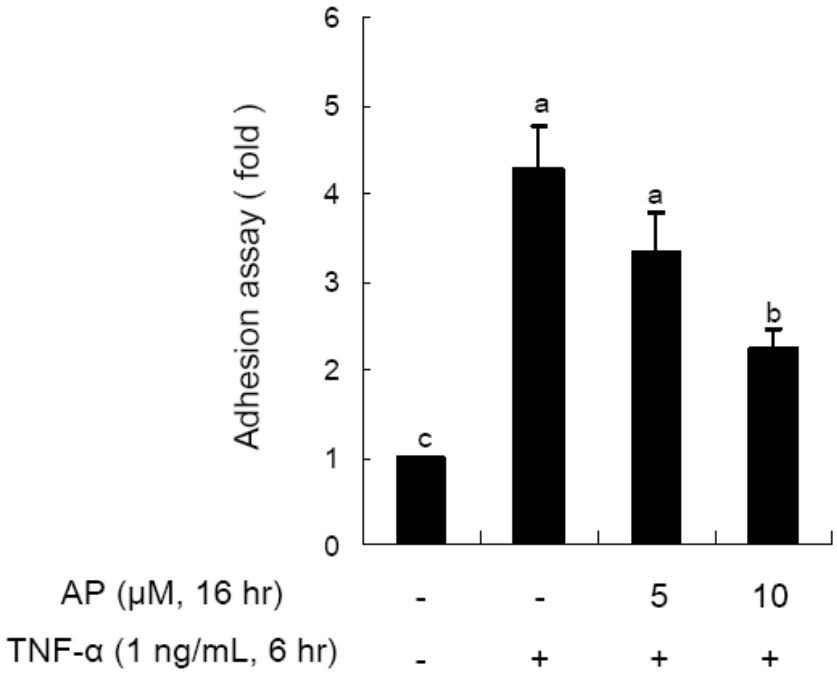

Figure 6. Andrographolide decreases TNF-α-induced HL-60 cell adhesion. Cells were pretreated with andrographolide for 16 h before being challenged with 1 ng/mL TNF-α for an additional 6 h. The levels in control cells were set at 1. Values are means ± SD of three independent experiments. Values not sharing an alphabetic letter are significantly different ($p < 0.05$).

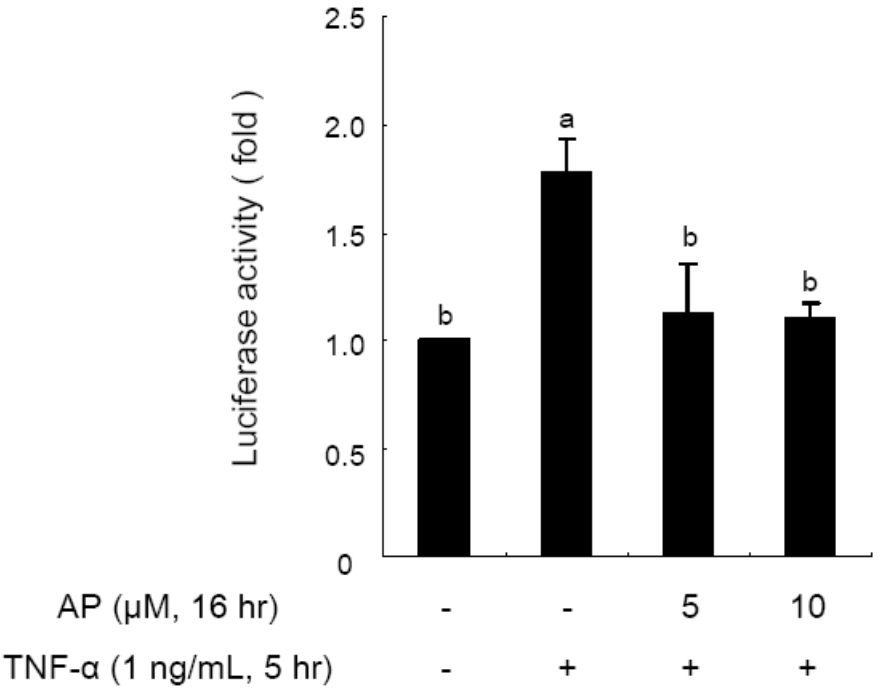

Figure 7. Andrographolide inhibits TNF-α-induced ICAM-1 promoter activity in EA.hy926 cells. Cells transfected with the pIC339 luciferase expression vector were pretreated with andrographolide for 16 h followed by incubation with TNF-α for an additional 5 h. The cells were then lysed and analyzed for luciferase activity. Luciferase activity was assayed as described in Materials and Methods. Induction is shown as an increase in the normalized luciferase activity in the treated cells relative to the control. Values are means ± SD of three independent experiments. Values not sharing an alphabetic letter are significantly different ($p < 0.05$).

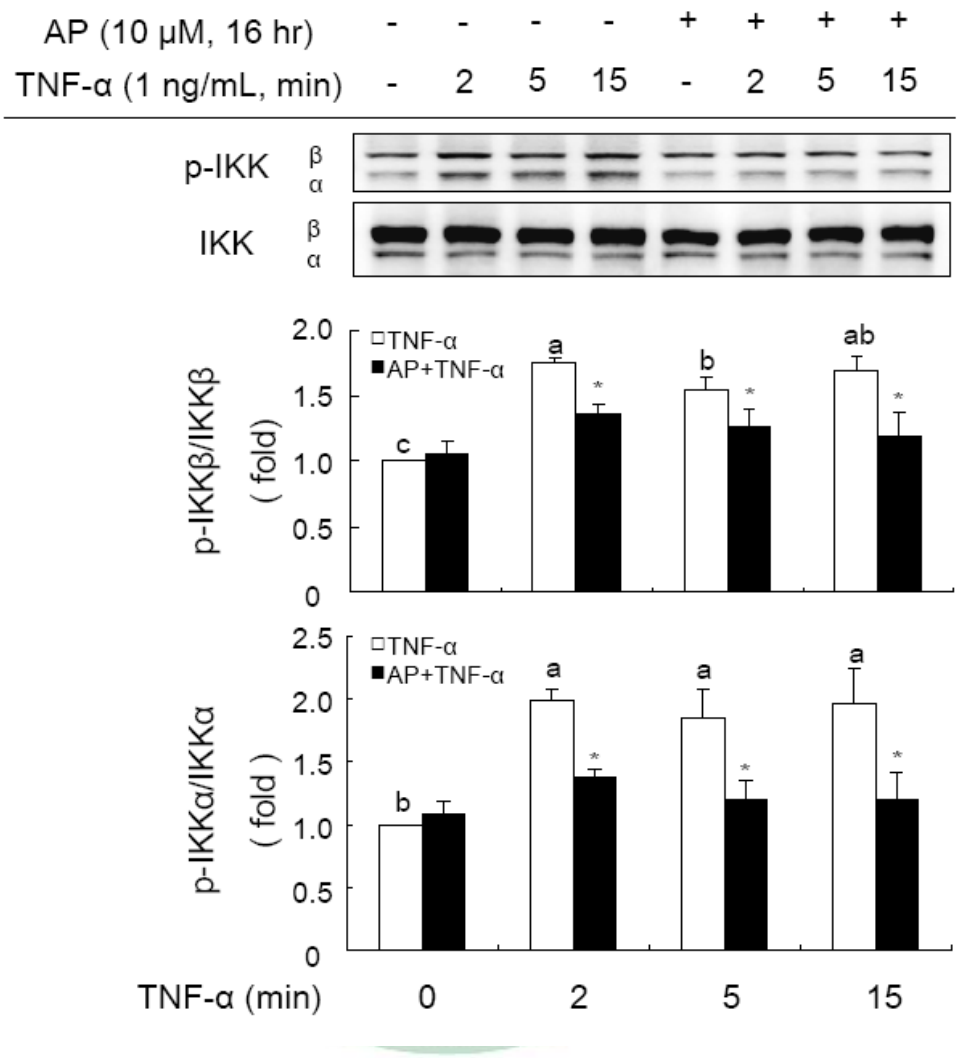

Figure 8. Andrographolide attenuates TNF-α-induced IKKα/β phosphorylation in EA.hy926 cells. Cells were pretreated with 10 μM andrographolide for 16 h followed by incubation with 1 ng/mL TNF-α for the various time periods. Aliquots of total protein (20 μg) were used for Western blot analysis. Fold is shown as an increase in the normalized phorphorylation in the treated cells relative to the control. Values are means ± SD of three independent experiments. Values not sharing an alphabetic letter are significantly different ($p < 0.05$). * $p < 0.05$ indicates significant effect of andrographolide on TNF-α-induced IKKα/β phosphorylation.

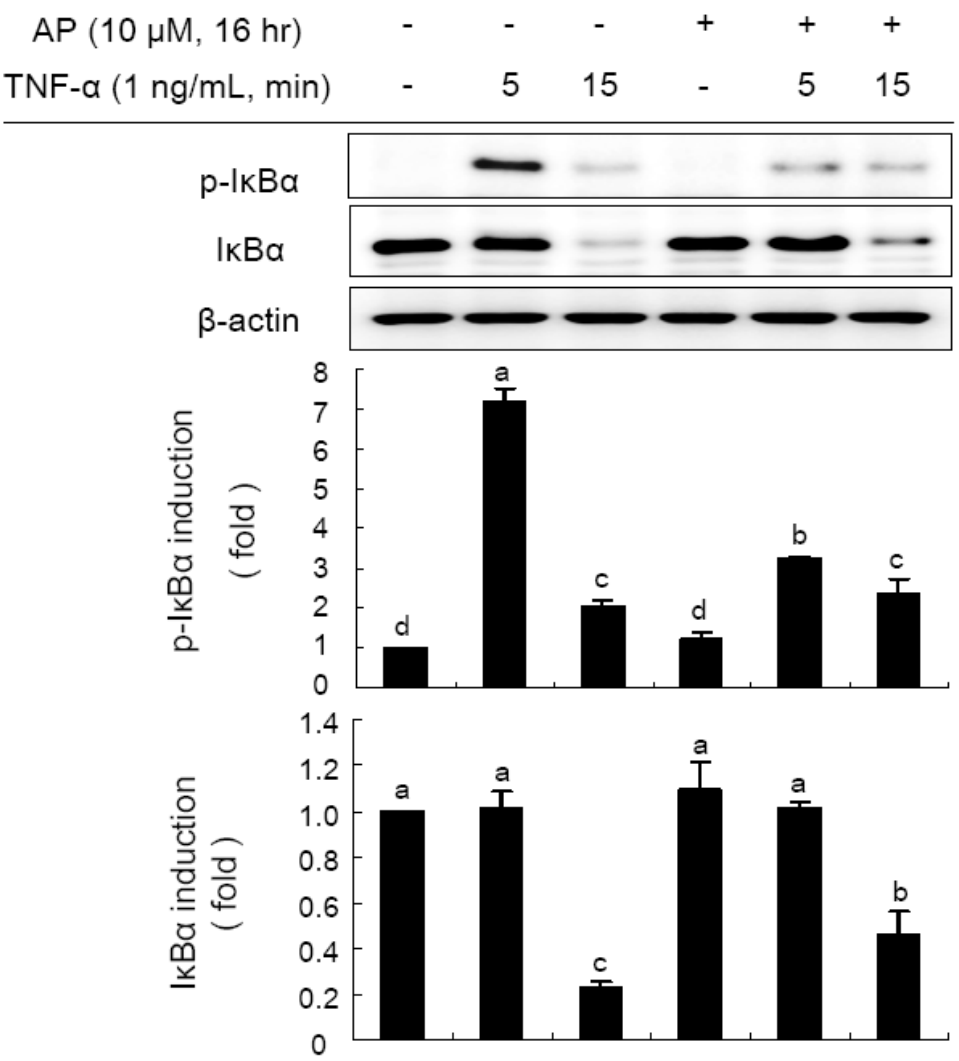

Figure 9. AP diminishes TNF-α-induced IκBα phosphorylation and degradation in EA.hy926 cells. Cells were pretreated with 10 μM andrographolide for 16 h followed by incubation with 1 ng/mL TNF-α for various time periods. Aliquots of total protein (20 μg) were used for Western blot analysis. The levels in control cells were set at 1. Values are means ± SD of three independent experiments. Values not sharing an alphabetic letter are significantly different ($p < 0.05$).

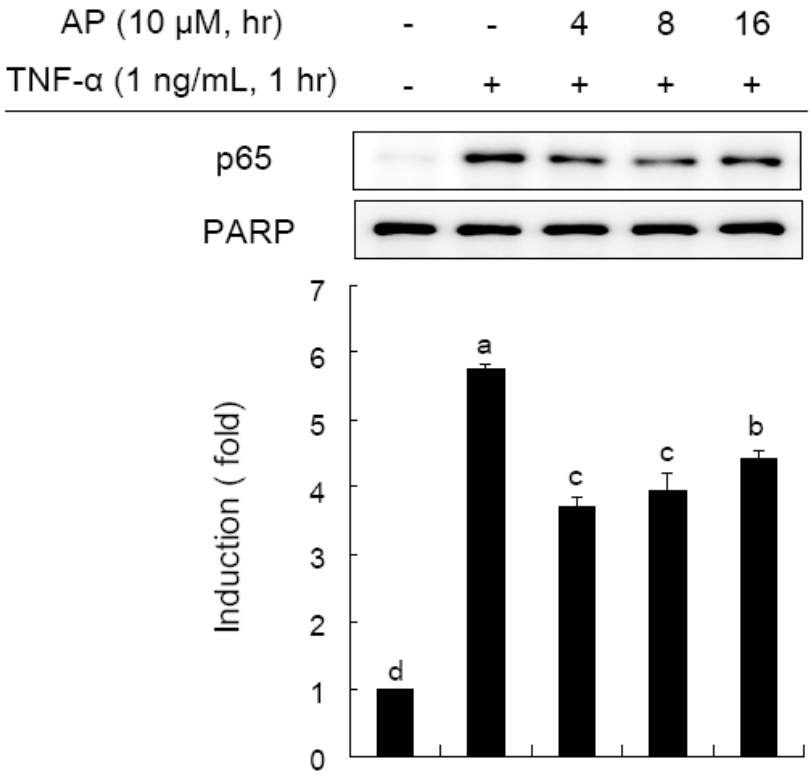

Figure 10. Andrographolide decreases TNF-α-induced p65 nuclear translocation in EA.hy926 cells. Cells were pretreated with 10 μM andrographolide for various time periods followed by incubation with 1 ng/mL TNF-α for an additional 1 h. Nuclear extracts (10 μg) were used for Western blot analysis. The levels in control cells were set at 1. Values are means ± SD of three independent experiments. Values not sharing an alphabetic letter are significantly different ($p < 0.05$).

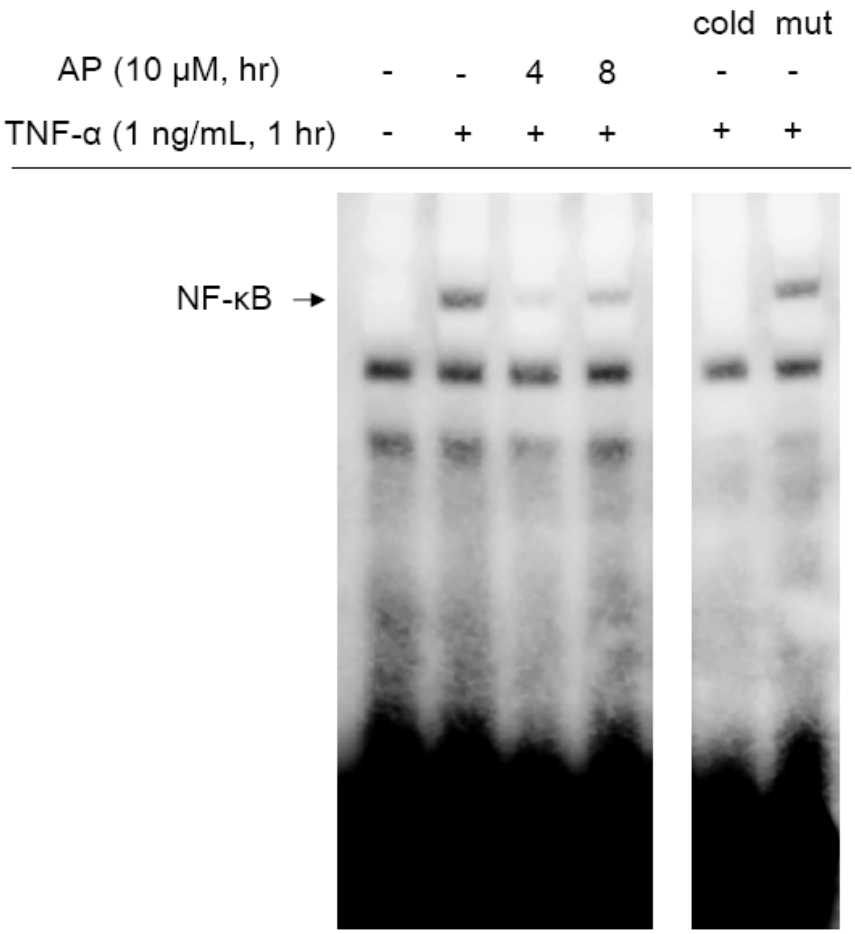

Figure 11. Effect of andrographolide on TNF-α-induced NF-κB-DNA binding activity in EA.hy926 cells. Cells were pretreated with 10 μM andrographolide for various time periods followed by incubation with 1 ng/mL TNF-α for an additional 1 h. Aliquots of nuclear extracts (10 μg) were used for EMSA. One representative experiment out of three independent experiments is shown.

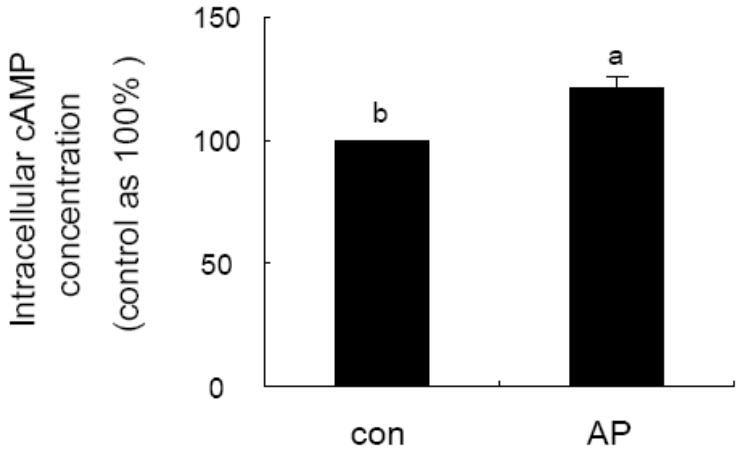

Figure 12. Effect of andrographolide on intracellular cAMP concentration in EA.hy926 cells. Cells were treated with 10 μM andrographolide for 30 min. Values are means ± SD of three independent experiments. Values not sharing an alphabetic letter are significantly different ($p < 0.05$).

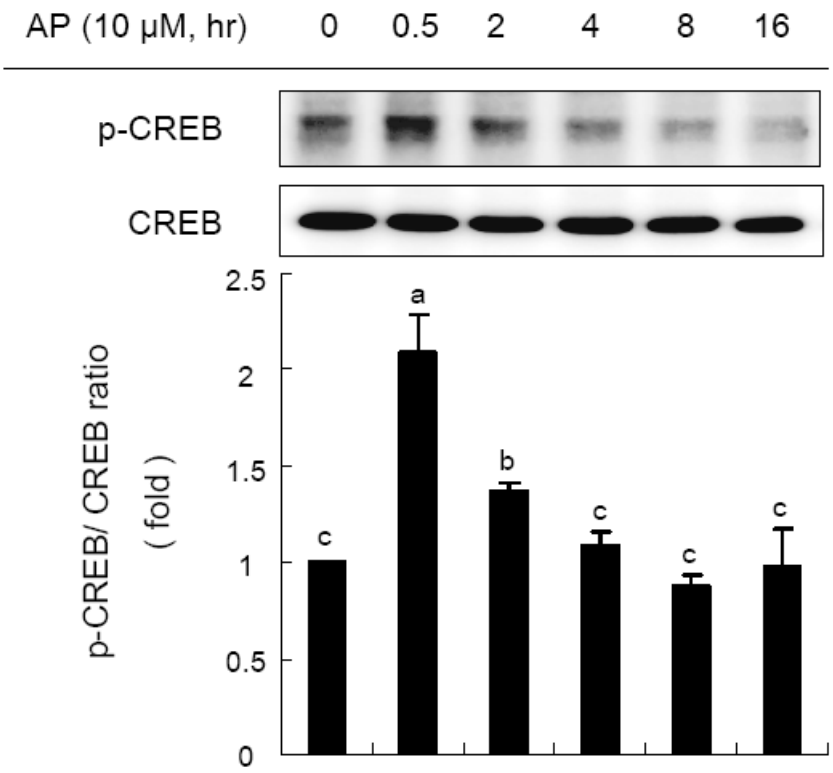

Figure 13. Andrographolide induces CREB phosphorylation in EA.hy926 cells. Cells were treated with 10 μM andrographolide for various time periods. Nuclear extracts (15 μg) were used for Western blot analysis. The levels in control cells were set at 1. Values are means ± SD of three independent experiments. Values not sharing an alphabetic letter are significantly different ($p < 0.05$).

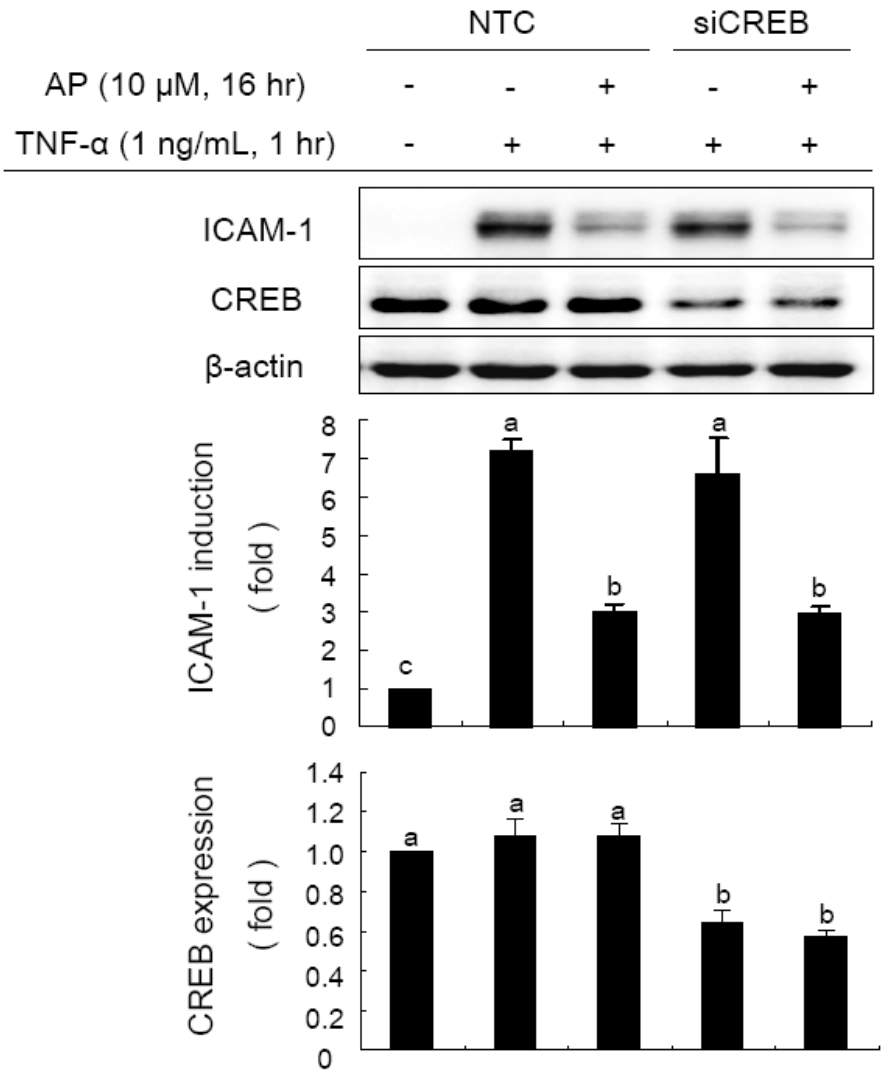

Figure 14. Effect of CREB siRNA on andrographolide inhibition of TNF-α-induced ICAM-1 expression in EA.hy926 cells. A CREB siRNA system was used to silence CREB mRNA in cells and to create an siRNA knockdown EA.hy926 cell model. Eight h after transfection, cells were pretreated with 10 μM andrographolide for 16 h followed by incubation with 1 ng/mL TNF-α for an additional 6 h. Aliquots of total protein (20 μg) were used for Western blot analysis. The levels in control cells were set at 1. Values are means ± SD of three independent experiments. Values not sharing an alphabetic letter are significantly different ($p < 0.05$). One representative immunoblot from three independent experiments is shown.

Discussion

In previous studies, andrographolide has been reported to have diverse properties including anti-inflammatory, anti-cancer, anti-viral, anti-oxidative, anti-hyperglycemic, and hepato-protective (Akowuah et al., 2008; Chandrasekaran et al., 2010; Chen et al., 2009; Qi et al., 2007; Singha et al., 2007; Yu et al., 2003). Atherosclerosis is an inflammatory response, and adhesion molecules were involved in atherosclerotic progression (Reiss and Engelhardt, 1999). We examined whether andrographolide inhibits TNF-α-induced ICAM-1 expression and the possible mechanisms involved. In the present study, TNF-α-induced both protein and mRNA levels of ICAM-1 was significantly inhibited by 10 μM andrographolide (Figure 3 and 4), and the results were consistent with that reported by Habtemariam (1998). These results suggest that andrographolide negatively regulates ICAM-1 expression at transcriptional level. The expression of adhesion molecule including ICAM-1 on the surface of endothelial cells is required for the firm adhesion of rolling monocytes (Kadono et al., 2002; Lehmann et al., 2003). It was shown that andrographolide reduced TNF-α-induced ICAM-1 expression on cell surfaces and monocyte adhesion (Figure 5 and 6). Based on the results, attenuation of ICAM-1 expression on cell surfaces plays an important role in the anti-monocyte adhesion.

There are a number of signaling pathways involved in TNF-α-mediated responses. They are IKK/NF-κB (Spiecker et al., 2002), MAPK (Clark et al., 2008; Hung et al., 2008), PI3K/Akt (Oh and Kwon, 2009), PKC (Min et al., 2005), and JAK/STAT (Kim et al., 2007). In addition to transcription factor NF-κB, AP-1 and STAT were considered to be involved in TNF-α-induced inflammatory gene

expression (Do et al., 2009; Wang et al., 2010). NF-κB is one kind of transcription factor which can be activated by TNF-α, ox-LDL, LPS, and other stimuli. The activation of NF-κB was modulated by IKK and IκBα (Sakurai et al., 2003).

Many phytochemicals have been shown to reduce inflammation through blocking NF-κB activation. For example, curcumin decreased the expression of ICAM-1, MCP-1, and IL-6 induced by TNF-α (Kim et al., 2007); incensole acetate reduced inflammation in the mouse paw model (Moussaieff et al., 2007); phloretin suppressed expression of endothelial adhesion molecules and reduced activation of human platelets (Stangl et al., 2005); and both lycopene and carnosol inhibited TNF-α-induced endothelial ICAM-1 expression and monocyte adhesion (Hung et al., 2008; Lian et al., 2010). These effects were attributed to the inhibition of NF-κB activation. In our study, we observed that TNF-α induced ICAM-1 promoter activity and this effect was abolished by 5 and 10 μM andrographolide (Figure 7). It was considered that the effect of andrographolide acts through the inhibition of NF-κB activation. To investigate whether IKK/NF-κB pathway was involved in the inhibition by andrographolide, IKKα/β phosphorylation, IκBα phosphorylation and degradation, p65 content in nucleus, and DNA binding activity of NF-κB were analyzed. Our data disclose that andrographolide inhibits TNF-α-induced IKKα/β phosphorylation (Figure 8), and reduces the phosphorylation and degradation of IκBα (Figure 9), p65 nuclear translocation (Figure 10), and DNA binding activity of NF-κB (Figure 11). Thereby, our results demonstrate that IKK is an andrograpjolide target in the NF-κB pathway. The inhibition of IKK/NF-κB signaling pathway by andrographolide was also found in human bronchial epithelial cells (Bao et al., 2009).

Additionally, several lines of evidence suggest that cAMP/PKA/CREB signaling pathway negatively regulates NF-κB-mediated transcription. Cilostazol, which increased intracellular cAMP level, inhibited THP-1cells adhesion to HUVECs (Mori et al., 2007). In human airway smooth muscle cells, pretreatment with forskolin, dibutryl cAMP, or isoproterenol inhibited TNF-α-induced ICAM-1 and VCAM-1 expression (Panettieri et al., 1995). The suppression was considered to occur due to the competition for the limited amount of CBP between p65 and CREB. Parry and Mackman (1997) indicated that the inhibition by forskolin was promoted by overexpression of CREB and was attenuated by overexpression of CBP in HUVECs. In our previous study, treatment with 40 μM andrographolide for 30 min dramatically elevated intracellular cAMP concentration by 22-fold and induced phosphorylation of CREB in rat primary hepatocytes (Yang et al., 2010). In EA.hy926 cells, we also observed the cAMP enhancing effect of andrographolide (Figure 12 and 13), although the magnitude was not as large as that seen in rat primary hepatocytes (Yang et al., 2010). The different results in the two cell culture systems can be attributed to the dose of andrographolide used and the different cell models examined. The increased cAMP level and CREB phosphorylation in response to andrographolide may play a role in suppression of ICAM-1 expression. In order to demonstrate the role of CREB phosphorylation in ICAM-1 expression, knockdown of CREB by using CREB siRNA was performed. Results showed that the inhibitory effect of andrographolide on TNF-α-induced ICAM-1 expression was not affected by CREB silencing (Figure 14).

In summary, andrographolide inhibits TNF-α-inducedICAM-1 expression and monocyte adhesion in EA.hy926 cells and this effect may involve the suppression of IKK/NF-κB signaling pathway rather than CREB phosphorylation.

Conclusion

In the present study, we demonstrate that andrographolide inhibited TNF-α induced ICAM-1 expression and monocyte adhesion. This inhibition is at least partially through suppression of IKK/NF-κB signaling pathway exerted by andrographolide. The findings of this study are schematically presented in Figure 15.

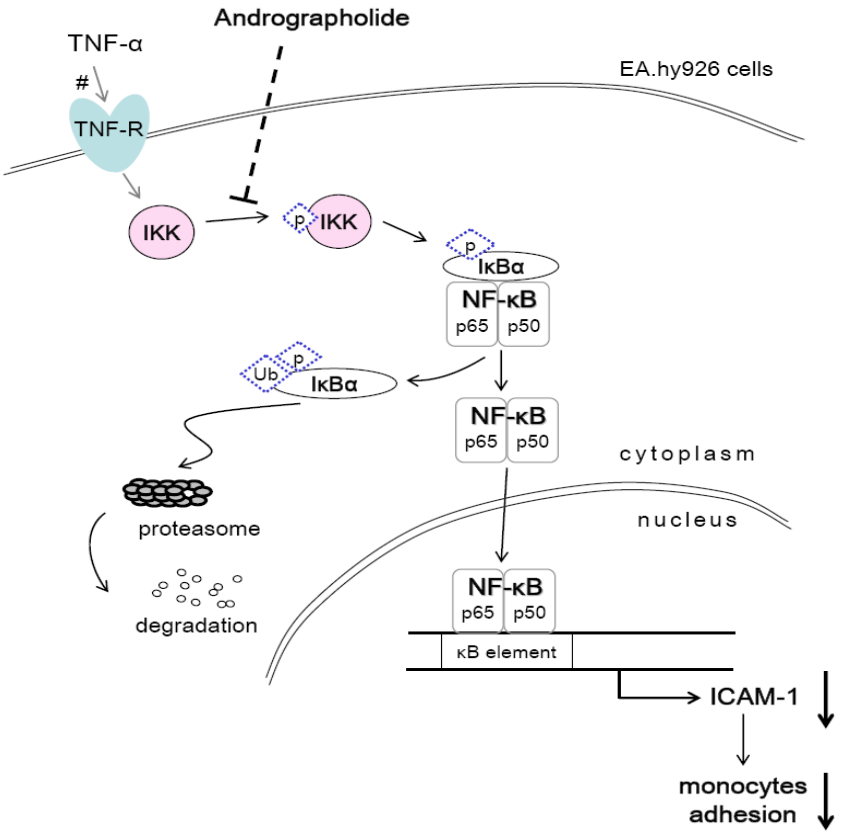

Figure 15. Model showing pathways that mediate the inhibition of expression of ICAM-1 and adhesion of HL-60 cells to EA.hy926 cells by andrographolide under inflammatory conditions. Andrographolide inhibits TNF-α-induced IKK activation, IκBα phosphorylation and degradation, p65 nuclear translocation, and DNA binding activity of NF-κB; eventually, suppresses ICAM-1 expression and monocyte adhesion. #(Mackay et al., 1993)

參考文獻

行政院衛生署 (2009). 死因統計統計表.

Abu-Ghefreh, A.A., Canatan, H., and Ezeamuzie, C.I. (2009). In vitro and in vivo anti-inflammatory effects of andrographolide. Int Immunopharmacol *9*, 313-318.

Akbarsha, M.A., Manivannan, B., Hamid, K.S., and Vijayan, B. (1990). Antifertility effect of Andrographis paniculata (Nees) in male albino rat. Indian J Exp Biol *28*, 421-426

Akowuah, G.A., Zhari, I., and Mariam, A. (2008). Analysis of urinary andrographolides and antioxidant status after oral administration of Andrographis paniculata leaf extract in rats. Food Chem Toxicol *46*, 3616-3620.

Audette, M., Larouche, L., Lussier, I., and Fugere, N. (2001). Stimulation of the ICAM-1 gene transcription by the peroxovanadium compound [bpV(Pic)] involves STAT-1 but not NF-kappa B activation in 293 cells. Eur J Biochem *268*, 1828-1836.

Balyasnikova, I.V., Pelligrino, D.A., Greenwood, J., Adamson, P., Dragon, S., Raza, H., and Galea, E. (2000). Cyclic adenosine monophosphate regulates the expression of the intercellular adhesion molecule and the inducible nitric oxide synthase in brain endothelial cells. J Cereb Blood Flow Metab *20*, 688-699.

Bao, Z., Guan, S., Cheng, C., Wu, S., Wong, S.H., Kemeny, D.M., Leung, B.P., and Wong, W.S. (2009). A novel antiinflammatory role for andrographolide in asthma via inhibition of the nuclear factor-kappaB pathway. Am J Respir Crit Care Med *179*, 657-665.

Berendji-Grun, D., Kolb-Bachofen, V., and Kroncke, K.D. (2001). Nitric oxide inhibits endothelial IL-1[beta]-induced ICAM-1 gene expression at the transcriptional level decreasing Sp1 and AP-1 activity. Mol Med *7*, 748-754.

Blankenberg, S., Barbaux, S., and Tiret, L. (2003). Adhesion molecules and atherosclerosis. Atherosclerosis *170*, 191-203.

Bonizzi, G., and Karin, M. (2004). The two NF-kappaB activation pathways and their role in innate and adaptive immunity. Trends Immunol *25*, 280-288.

Burgos, R.A., Caballero, E.E., Sanchez, N.S., Schroeder, R.A., Wikman, G.K., and Hancke, J.L. (1997). Testicular toxicity assessment of Andrographis paniculata dried extract in rats. J Ethnopharmacol *58*, 219-224

Chandrasekaran, C.V., Thiyagarajan, P., Sundarajan, K., Goudar, K.S., Deepak, M., Murali, B., Allan, J.J., and Agarwal, A. (2009). Evaluation of the genotoxic potential and acute oral toxicity of standardized extract of Andrographis paniculata (KalmCold). Food Chem Toxicol *47*, 1892-1902

Chandrasekaran, C.V., Gupta, A., and Agarwal, A. (2010). Effect of an extract of Andrographis paniculata leaves on inflammatory and allergic mediators in vitro. J Ethnopharmacol *129*, 203-207.

Chen, J.X., Xue, H.J., Ye, W.C., Fang, B.H., Liu, Y.H., Yuan, S.H., Yu, P., and Wang, Y.Q. (2009). Activity of andrographolide and its derivatives against influenza virus in vivo and in vitro. Biol Pharm Bull *32*, 1385-1391.

Chen, L.F., and Greene, W.C. (2003). Regulation of distinct biological activities of the NF-kappaB transcription factor complex by acetylation. J Mol Med *81*, 549-557.

Chen, L.F., and Greene, W.C. (2004). Shaping the nuclear action of NF-kappaB. Nat Rev *5*, 392-401.

Cheng, C.Y., Su, S.Y., Tang, N.Y., Ho, T.Y., Chiang, S.Y., and Hsieh, C.L. (2008). Ferulic acid provides neuroprotection against oxidative stress-related apoptosis after cerebral ischemia/reperfusion injury by inhibiting ICAM-1 mRNA expression in rats. Brain Res *1209*, 136-150.

Cheng, W.L., Lii, C.K., Chen, H.W., Lin, T.H., and Liu, K.L. (2004). Contribution of conjugated linoleic acid to the suppression of inflammatory responses through the regulation of the NF-kappaB pathway. J Agric Food Chem *52*, 71-78.

Chiou, W.F., Chen, C.F., and Lin, J.J. (2000). Mechanisms of suppression of inducible nitric oxide synthase (iNOS) expression in RAW 264.7 cells by andrographolide. Br J Pharmacol *129*, 1553-1560.

Clark, P.R., Pober, J.S., and Kluger, M.S. (2008). Knockdown of TNFR1 by the sense strand of an ICAM-1 siRNA: dissection of an off-target effect. Nucleic Acids Res *36*, 1081-1097.

Coon, J.T., and Ernst, E. (2004). Andrographis paniculata in the treatment of upper respiratory tract infections: a systematic review of safety and efficacy. Planta Med *70*, 293-298.

Cui, J., Chen, P.B., Yang, X.F., and Huang, H. (2010). Effect of the simple acupoint catgut embedding on the expression of ICAM-1, NF-kappaB and airway inflammation in rats with asthma. Zhongguo Zhen Jiu *30*, 141-145.

Do, H., Pyo, S., and Sohn, E.H. (2009). Suppression of iNOS expression by fucoidan is mediated by regulation of p38 MAPK, JAK/STAT, AP-1 and IRF-1, and depends on up-regulation of scavenger receptor B1 expression in TNF-alpha- and IFN-gamma-stimulated C6 glioma cells. J Nutr Biochem *21*, 671-679

Du, X.D., Zhang, S., Cao, Y., and Nie, H. (2009). Effect of felodipine on the expression of NF-kappaB in rat model of atherosclerosis. Sichuan Da Xue Xue Bao Yi Xue Ban *40*, 826-828.

Eriksson, E.E., Xie, X., Werr, J., Thoren, P., and Lindbom, L. (2001). Importance of primary capture and L-selectin-dependent secondary capture in leukocyte accumulation in inflammation and atherosclerosis in vivo. J Exp Med *194*, 205-218.

Galkina, E., Kadl, A., Sanders, J., Varughese, D., Sarembock, I.J., and Ley, K. (2006). Lymphocyte recruitment into the aortic wall before and during development of atherosclerosis is partially L-selectin dependent. J Exp Med *203*, 1273-1282.

Galkina, E., and Ley, K. (2007). Vascular adhesion molecules in atherosclerosis. Arterioscler Thromb Vasc Biol *27*, 2292-2301.

Gao, X., Belmadani, S., Picchi, A., Xu, X., Potter, B.J., Tewari-Singh, N., Capobianco, S., Chilian, W.M., and Zhang, C. (2007). Tumor necrosis factor-alpha induces endothelial dysfunction in Lepr(db) mice. Circulation *115*, 245-254.

Gareus, R., Kotsaki, E., Xanthoulea, S., van der Made, I., Gijbels, M.J., Kardakaris, R., Polykratis, A., Kollias, G., de Winther, M.P., and Pasparakis, M. (2008). Endothelial cell-specific NF-kappaB inhibition protects mice from atherosclerosis. Cell Metab *8*, 372-383.

Gerritsen, M.E., Williams, A.J., Neish, A.S., Moore, S., Shi, Y., and Collins, T. (1997). CREB-binding protein/p300 are transcriptional coactivators of p65. Proc Natl Acad Sci U S A *94*, 2927-2932.

Guo, S.Y., Li, D.Z., Li, W.S., Fu, A.H. and Zhang, L.F. (1988) Study of the toxicity of andrographolide in rabbits. J Beijing Med Univ *5*, 422-428.

Habtemariam, S. (1998). Andrographolide inhibits the tumour necrosis factor-alpha-induced upregulation of ICAM-1 expression and endothelial-monocyte adhesion. Phytother Res *12*, 37-40.

Hansson, G.K. (2005). Inflammation, atherosclerosis, and coronary artery disease. N Engl J Med *352*, 1685-1695.

Hansson, G.K. (2009). Inflammatory mechanisms in atherosclerosis. J Thromb Haemost *7 Suppl 1*, 328-331.

Hayden, M.S., and Ghosh, S. (2004). Signaling to NF-kappaB. Genes Dev *18*, 2195-2224.

Hidalgo, M.A., Romero, A., Figueroa, J., Cortes, P., Concha, II, Hancke, J.L., and Burgos, R.A. (2005). Andrographolide interferes with binding of nuclear factor-kappaB to DNA in HL-60-derived neutrophilic cells. Br J Pharmacol *144*, 680-686.

Hou, J., Baichwal, V., and Cao, Z. (1994). Regulatory elements and transcription factors controlling basal and cytokine-induced expression of the gene encoding intercellular adhesion molecule 1. Proc Natl Acad Sci U S A *91*, 11641-11645.

Huang, W.C., and Chen, C.C. (2005). Akt phosphorylation of p300 at Ser-1834 is essential for its histone acetyltransferase and transcriptional activity. Mol Cell Biol *25*, 6592-6602.

Hung, C.F., Huang, T.F., Chen, B.H., Shieh, J.M., Wu, P.H., and Wu, W.B. (2008). Lycopene inhibits TNF-alpha-induced endothelial ICAM-1 expression and monocyte-endothelial adhesion. Eur J Pharmacol *586*, 275-282.

Hynes, R.O. (2002). Integrins: bidirectional, allosteric signaling machines. Cell *110*, 673-687.

Jaruchotikamol, A., Jarukamjorn, K., Sirisangtrakul, W., Sakuma, T., Kawasaki, Y., and Nemoto, N. (2007). Strong synergistic induction of CYP1A1 expression by andrographolide plus typical CYP1A inducers in mouse hepatocytes. Toxicol Appl Pharmacol *224*, 156-162.

Jiang, C.G., Li, J.B., Liu, F.R., Wu, T., Yu, M., and Xu, H.M. (2007). Andrographolide inhibits the adhesion of gastric cancer cells to endothelial cells by blocking E-selectin expression. Anticancer Res *27*, 2439-2447.

Kadono, T., Venturi, G.M., Steeber, D.A., and Tedder, T.F. (2002). Leukocyte rolling velocities and migration are optimized by cooperative L-selectin and intercellular adhesion molecule-1 functions. J Immunol *169*, 4542-4550.

Kaufmann, B.A., Sanders, J.M., Davis, C., Xie, A., Aldred, P., Sarembock, I.J., and Lindner, J.R. (2007). Molecular imaging of inflammation in atherosclerosis with targeted ultrasound detection of vascular cell adhesion molecule-1. Circulation *116*, 276-284.

Kim, Y.S., Ahn, Y., Hong, M.H., Joo, S.Y., Kim, K.H., Sohn, I.S., Park, H.W., Hong, Y.J., Kim, J.H., Kim, W.*, et al.* (2007). Curcumin attenuates inflammatory responses of TNF-alpha-stimulated human endothelial cells. J Cardiovasc Pharmacol *50*, 41-49.

Koteswara Rao, Y., Vimalamma, G., Rao, C.V., and Tzeng, Y.M. (2004). Flavonoids and andrographolides from Andrographis paniculata. Phytochemistry *65*, 2317-2321.

Kumar, S., Sharma, A., Madan, B., Singhal, V., and Ghosh, B. (2007). Isoliquiritigenin inhibits IkappaB kinase activity and ROS generation to block TNF-alpha induced expression of cell adhesion molecules on human endothelial cells. Biochem Pharmacol *73*, 1602-1612.

Lawson, C., and Wolf, S. (2009). ICAM-1 signaling in endothelial cells. Pharmacol Rep *61*, 22-32.

Lee, Y.C., Lin, H.H., Hsu, C.H., Wang, C.J., Chiang, T.A., and Chen, J.H. (2010). Inhibitory effects of andrographolide on migration and invasion in human non-small cell lung cancer A549 cells via down-regulation of PI3K/Akt signaling pathway. Eur J Pharmacol *632*, 23-32.

Lehmann, J.C., Jablonski-Westrich, D., Haubold, U., Gutierrez-Ramos, J.C., Springer, T., and Hamann, A. (2003). Overlapping and selective roles of endothelial intercellular adhesion molecule-1 (ICAM-1) and ICAM-2 in lymphocyte trafficking. J Immunol *171*, 2588-2593.

Li, D., Liu, L., Chen, H., Sawamura, T., and Mehta, J.L. (2003). LOX-1, an oxidized LDL endothelial receptor, induces CD40/CD40L signaling in human coronary artery endothelial cells. Arterioscler Thromb Vasc Biol *23*, 816-821.

Li, J., Luo, L., Wang, X., Liao, B., and Li, G. (2009). Inhibition of NF-kappaB expression and allergen-induced airway inflammation in a mouse allergic asthma model by andrographolide. Cell Mol Immunol *6*, 381-385.

Lian, K.C., Chuang, J.J., Hsieh, C.W., Wung, B.S., Huang, G.D., Jian, T.Y., and Sun, Y.W. (2010). Dual mechanisms of NF-kappaB inhibition in carnosol-treated endothelial cells. Toxicol Appl Pharmacol *245*, 21-35.

Lin, C.W., Chen, L.J., Lee, P.L., Lee, C.I., Lin, J.C., and Chiu, J.J. (2007). The inhibition of TNF-alpha-induced E-selectin expression in endothelial cells via the JNK/NF-kappaB pathways by highly N-acetylated chitooligosaccharides. Biomaterials *28*, 1355-1366.

Mackay, F., Loetscher, H., Stueber, D., Gehr, G., and Lesslauer, W. (1993). Tumor necrosis factor alpha (TNF-alpha)-induced cell adhesion to human endothelial cells is under dominant control of one TNF receptor type, TNF-R55. J Exp Med *177*, 1277-1286.

Madamanchi, N.R., Vendrov, A., and Runge, M.S. (2005). Oxidative stress and vascular disease. Arterioscler Thromb Vasc Biol *25*, 29-38.

Maiti, K., Mukherjee, K., Murugan, V., Saha, B.P., and Mukherjee, P.K. (2010). Enhancing bioavailability and hepatoprotective activity of andrographolide from Andrographis paniculata, a well-known medicinal food, through its herbosome. J Sci Food Agric *90*, 43-51.

Matheny, H.E., Deem, T.L., and Cook-Mills, J.M. (2000). Lymphocyte migration through monolayers of endothelial cell lines involves VCAM-1 signaling via endothelial cell NADPH oxidase. J Immunol *164*, 6550-6559.

Meager, A. (1999). Cytokine regulation of cellular adhesion molecule expression in inflammation. Cytokine Growth Factor Rev *10*, 27-39.

Meagher, L., Mahiouz, D., Sugars, K., Burrows, N., Norris, P., Yarwood, H., Becker-Andre, M., and Haskard, D.O. (1994). Measurement of mRNA for E-selectin, VCAM-1 and ICAM-1 by reverse transcription and the polymerase chain reaction. J Immunol Methods *175*, 237-246.

Michael, L.F., Asahara, H., Shulman, A.I., Kraus, W.L., and Montminy, M. (2000). The phosphorylation status of a cyclic AMP-responsive activator is modulated via a chromatin-dependent mechanism. Mol Cell Biol *20*, 1596-1603.

Min, J.K., Kim, Y.M., Kim, S.W., Kwon, M.C., Kong, Y.Y., Hwang, I.K., Won, M.H., Rho, J., and Kwon, Y.G. (2005). TNF-related activation-induced cytokine enhances leukocyte adhesiveness: induction of ICAM-1 and VCAM-1 via TNF receptor-associated factor and protein kinase C-dependent NF-kappaB activation in endothelial cells. J Immunol *175*, 531-540.

Mori, D., Ishii, H., Kojima, C., Nitta, N., Nakajima, K., and Yoshida, M. (2007). Cilostazol inhibits monocytic cell adhesion to vascular endothelium via upregulation of cAMP. J Atheroscler Thromb *14*, 213-218.

Moussaieff, A., Shohami, E., Kashman, Y., Fride, E., Schmitz, M.L., Renner, F., Fiebich, B.L., Munoz, E., Ben-Neriah, Y., and Mechoulam, R. (2007). Incensole acetate, a novel anti-inflammatory compound isolated from Boswellia resin, inhibits nuclear factor-kappa B activation. Mol Pharmacol *72*, 1657-1664.

Moynagh, P.N. (2005). The NF-kappaB pathway. J Cell Sci *118*, 4589-4592.

Newman, W.H., Zhang, L.M., Lee, D.H., Dalton, M.L., Warejcka, D.J., Castresana, M.R., and Leeper-Woodford, S.K. (1998). Release of tumor necrosis factor-alpha from coronary smooth muscle: activation of NF-kappaB and inhibition by elevated cyclic AMP. The J Surg Res *80*, 129-135.

Newton, J.P., Buckley, C.D., Jones, E.Y., and Simmons, D.L. (1997). Residues on both faces of the first immunoglobulin fold contribute to homophilic binding sites of PECAM-1/CD31. J Biol Chem *272*, 20555-20563.

Oh, J.H., and Kwon, T.K. (2009). Withaferin A inhibits tumor necrosis factor-alpha-induced expression of cell adhesion molecules by inactivation of Akt and NF-kappaB in human pulmonary epithelial cells. Int Immunopharmacol *9*, 614-619.

Oh, J.H., Park, E.J., Park, J.W., Lee, J., Lee, S.H., and Kwon, T.K. (2010). A novel cyclin-dependent kinase inhibitor down-regulates tumor necrosis factor-alpha (TNF-alpha)-induced expression of cell adhesion molecules by inhibition of NF-kappaB activation in human pulmonary epithelial cells. Int Immunopharmacol *10*, 572-579.

Ohta, H., Wada, H., Niwa, T., Kirii, H., Iwamoto, N., Fujii, H., Saito, K., Sekikawa, K., and Seishima, M. (2005). Disruption of tumor necrosis factor-alpha gene diminishes the development of atherosclerosis in ApoE-deficient mice. Atherosclerosis *180*, 11-17.

Ollivier, V., Parry, G.C., Cobb, R.R., de Prost, D., and Mackman, N. (1996). Elevated cyclic AMP inhibits NF-kappaB-mediated transcription in human monocytic cells and endothelial cells. J Biol Chem *271*, 20828-20835.

Panettieri, R.A., Jr., Lazaar, A.L., Pure, E., and Albelda, S.M. (1995). Activation of cAMP-dependent pathways in human airway smooth muscle cells inhibits TNF-alpha-induced ICAM-1 and VCAM-1 expression and T lymphocyte adhesion. J Immunol *154*, 2358-2365.

Parker, D., Rivera, M., Zor, T., Henrion-Caude, A., Radhakrishnan, I., Kumar, A., Shapiro, L.H., Wright, P.E., Montminy, M., and Brindle, P.K. (1999). Role of secondary structure in discrimination between constitutive and inducible activators. Mol Cell Biol *19*, 5601-5607.

Parry, G.C., and Mackman, N. (1997). Role of cyclic AMP response element-binding protein in cyclic AMP inhibition of NF-kappaB-mediated transcription. J Immunol *159*, 5450-5456.

Pekthong, D., Blanchard, N., Abadie, C., Bonet, A., Heyd, B., Mantion, G., Berthelot, A., Richert, L., and Martin, H. (2009). Effects of Andrographis paniculata extract and Andrographolide on hepatic cytochrome P450 mRNA expression and monooxygenase activities after in vivo administration to rats and in vitro in rat and human hepatocyte cultures. Chem Biol Interact *179*, 247-255.

Pekthong, D., Martin, H., Abadie, C., Bonet, A., Heyd, B., Mantion, G., and Richert, L. (2008). Differential inhibition of rat and human hepatic cytochrome P450 by Andrographis paniculata extract and andrographolide. J Ethnopharmacol *115*, 432-440.

Perkins, N.D. (2007). Integrating cell-signalling pathways with NF-kappaB and IKK function. Nat Rev *8*, 49-62.

Poolsup, N., Suthisisang, C., Prathanturarug, S., Asawamekin, A., and Chanchareon, U. (2004). Andrographis paniculata in the symptomatic treatment of uncomplicated upper respiratory tract infection: systematic review of randomized controlled trials. J Clin Pharm Ther *29*, 37-45.

Qi, C.L., Wang, L.J., and Zhou, X.L. (2007). [Advances in study on anti-tumor mechanism of andrographolide]. Zhongguo Zhong yao za zhi *32*, 2095-2097.

Qin, L.H., Kong, L., Shi, G.J., Wang, Z.T., and Ge, B.X. (2006). Andrographolide inhibits the production of TNF-alpha and interleukin-12 in lipopolysaccharide-stimulated macrophages: role of mitogen-activated protein kinases. Biol Pharm Bull *29*, 220-224.

Rajagopal, S., Kumar, R.A., Deevi, D.S., Satyanarayana, C., and Rajagopalan, R. (2003). Andrographolide, a potential cancer therapeutic agent isolated from Andrographis paniculata. J Exp Ther Oncol *3*, 147-158.

Redmond, E.M., Morrow, D., Kundimi, S., Miller-Graziano, C.L., and Cullen, J.P. (2009). Acetaldehyde stimulates monocyte adhesion in a P-selectin- and TNFalpha-dependent manner. Atherosclerosis *204*, 372-380.

Reiss, Y., and Engelhardt, B. (1999). T cell interaction with ICAM-1-deficient endothelium in vitro: transendothelial migration of different T cell populations is mediated by endothelial ICAM-1 and ICAM-2. Int Immunol *11*, 1527-1539.

Roebuck, K.A., and Finnegan, A. (1999). Regulation of intercellular adhesion molecule-1 (CD54) gene expression. J Leukoc Biol *66*, 876-888.

Rothwarf, D.M., Zandi, E., Natoli, G., and Karin, M. (1998). IKK-gamma is an essential regulatory subunit of the IkappaB kinase complex. Nature *395*, 297-300.

Sakurai, H., Suzuki, S., Kawasaki, N., Nakano, H., Okazaki, T., Chino, A., Doi, T., and Saiki, I. (2003). Tumor necrosis factor-alpha-induced IKK phosphorylation of NF-kappaB p65 on serine 536 is mediated through the TRAF2, TRAF5, and TAK1 signaling pathway. J Biol Chem *278*, 36916-36923.

Satyanarayana, C., Deevi, D.S., Rajagopalan, R., Srinivas, N., and Rajagopal, S. (2004). DRF 3188 a novel semi-synthetic analog of andrographolide: cellular response to MCF 7 breast cancer cells. BMC cancer *4*, 26-33.

Shames, B.D., McIntyre, R.C., Jr., Bensard, D.D., Pulido, E.J., Selzman, C.H., Reznikov, L.L., Harken, A.H., and Meng, X. (2001). Suppression of tumor necrosis factor alpha production by cAMP in human monocytes: dissociation with mRNA level and independent of interleukin-10. J Surg Res *99*, 187-193.

Sheeja, K., Guruvayoorappan, C., and Kuttan, G. (2007). Antiangiogenic activity of Andrographis paniculata extract and andrographolide. Int Immunopharmacol *7*, 211-221.

Sheeja, K., and Kuttan, G. (2007). Activation of cytotoxic T lymphocyte responses and attenuation of tumor growth in vivo by Andrographis paniculata extract and andrographolide. Immunopharmacol and Immunotoxicol *29*, 81-93.

Shen, Y.C., Chen, C.F., and Chiou, W.F. (2002). Andrographolide prevents oxygen radical production by human neutrophils: possible mechanism(s) involved in its anti-inflammatory effect. Br J Pharmacol *135*, 399-406.

Singha, P.K., Roy, S., and Dey, S. (2007). Protective activity of andrographolide and arabinogalactan proteins from Andrographis paniculata Nees. against ethanol-induced toxicity in mice. J Ethnopharmacol *111*, 13-21.

Son, E.W., Rhee, D.K., and Pyo, S. (2006). Gamma-irradiation-induced intercellular adhesion molecule-1 (ICAM-1) expression is associated with catalase: activation of Ap-1 and JNK. J Toxicol Environ Health *69*, 2137-2155.

Spasov, A.A., Ostrovskij, O.V., Chernikov, M.V., and Wikman, G. (2004). Comparative controlled study of Andrographis paniculata fixed combination, Kan Jang and an Echinacea preparation as adjuvant, in the treatment of uncomplicated respiratory disease in children. Phytother Res *18*, 47-53.

Spiecker, M., Lorenz, I., Marx, N., and Darius, H. (2002). Tranilast inhibits cytokine-induced nuclear factor kappaB activation in vascular endothelial cells. Mol Pharmacol *62*, 856-863.

Stangl, V., Lorenz, M., Ludwig, A., Grimbo, N., Guether, C., Sanad, W., Ziemer, S., Martus, P., Baumann, G., and Stangl, K. (2005). The flavonoid phloretin suppresses stimulated expression of endothelial adhesion molecules and reduces activation of human platelets. J Nutr *135*, 172-178.

Sun, Z., and Andersson, R. (2002). NF-kappaB activation and inhibition: a review. Shock *18*, 99-106.

Takahashi, N., Tetsuka, T., Uranishi, H., and Okamoto, T. (2002). Inhibition of the NF-kappaB transcriptional activity by protein kinase A. Eur J Biochem *269*, 4559-4565.

Taylor, S.S., Buechler, J.A., and Yonemoto, W. (1990). cAMP-dependent protein kinase: framework for a diverse family of regulatory enzymes. Annu Rev Biochem *59*, 971-1005.

Thisoda, P., Rangkadilok, N., Pholphana, N., Worasuttayangkurn, L., Ruchirawat, S., and Satayavivad, J. (2006). Inhibitory effect of Andrographis paniculata extract and its active diterpenoids on platelet aggregation. Eur J Pharmacol *553*, 39-45.

Trivedi, N.P., Rawal, U.M., and Patel, B.P. (2007). Hepatoprotective effect of andrographolide against hexachlorocyclohexane-induced oxidative injury. Integr Cancer Ther *6*, 271-280.

Trivedi, N.P., Rawal, U.M., and Patel, B.P. (2009). Potency of andrographolide as an antitumor compound in BHC-induced liver damage. Integr Cancer Ther *8*, 177-189.

van de Stolpe, A., Caldenhoven, E., Stade, B.G., Koenderman, L., Raaijmakers, J.A., Johnson, J.P., and van der Saag, P.T. (1994). 12-O-tetradecanoylphorbol-13-acetate- and tumor necrosis factor alpha-mediated induction of intercellular adhesion molecule-1 is inhibited by dexamethasone. Functional analysis of the human intercellular adhesion molecular-1 promoter. J Biol Chem *269*, 6185-6192.

van de Stolpe, A., and van der Saag, P.T. (1996). Intercellular adhesion molecule-1. J Mol Med *74*, 13-33.

Visen, P.K., Shukla, B., Patnaik, G.K., and Dhawan, B.N. (1993). Andrographolide protects rat hepatocytes against paracetamol-induced damage. J Ethnopharmacol *40*, 131-136.

Vo, N., and Goodman, R.H. (2001). CREB-binding protein and p300 in transcriptional regulation. J Biol Chem *276*, 13505-13508.

Voraberger, G., Schafer, R., and Stratowa, C. (1991). Cloning of the human gene for intercellular adhesion molecule 1 and analysis of its 5'-regulatory region. Induction by cytokines and phorbol ester. J Immunol *147*, 2777-2786.

Wongkittipong, R., Prat, L., Damronglerd, S., and Gourdon, C. (2004). Solid-liquid extraction of andrographolide from plants-experimental study, kinetic reaction and model. Sep Purif Technol *40*, 147-154.

Xiao, N., Yin, M., Zhang, L., Qu, X., Du, H., Sun, X., Mao, L., Ren, G., Zhang, C., Geng, Y.*, et al.* (2009). Tumor necrosis factor-alpha deficiency retards early fatty-streak lesion by influencing the expression of inflammatory factors in apoE-null mice. Mol Genet Metab *96*, 239-244.

Yang, A.J., Li, C.C., Lu, C.Y., Liu, K.L., Tsai, C.W., Lii, C.K., and Chen, H.W. (2010). Activation of the cAMP/CREB/inducible cAMP early repressor pathway suppresses andrographolide-induced gene expression of the pi class of glutathione S-transferase in rat primary hepatocytes. J Agric Food Chem *58*, 1993-2000.

Ying, B., Yang, T., Song, X., Hu, X., Fan, H., Lu, X., Chen, L., Cheng, D., Wang, T., Liu, D.*, et al.* (2009). Quercetin inhibits IL-1 beta-induced ICAM-1 expression in pulmonary epithelial cell line A549 through the MAPK pathways. Mol Biol Rep *36*, 1825-1832.

Yu, B.C., Hung, C.R., Chen, W.C., and Cheng, J.T. (2003). Antihyperglycemic effect of andrographolide in streptozotocin-induced diabetic rats. Planta Med *69*, 1075-1079.

Yusuf-Makagiansar, H., Anderson, M.E., Yakovleva, T.V., Murray, J.S., and Siahaan, T.J. (2002). Inhibition of LFA-1/ICAM-1 and VLA-4/VCAM-1 as a therapeutic approach to inflammation and autoimmune diseases. Med Res Rev *22*, 146-167.

Zakeri, S.M., Meyer, H., Meinhardt, G., Reinisch, W., Schrattbauer, K., Knoefler, M., and Block, L.H. (2000). Effects of trovafloxacin on the IL-1-dependent activation of E-selectin in human endothelial cells in vitro. Immunopharmacology *48*, 27-34.

Zhang, X.F., and Tan, B.K. (2000). Anti-diabetic property of ethanolic extract of Andrographis paniculata in streptozotocin-diabetic rats. Acta Pharmacol Sin *21*, 1157-1164.

Zhao, F., He, E.Q., Wang, L., and Liu, K. (2008). Anti-tumor activities of andrographolide, a diterpene from Andrographis paniculata, by inducing apoptosis and inhibiting VEGF level. J Asian Nat Prod Res *10*, 467-473.

Zhou, Z., Connell, M.C., and MacEwan, D.J. (2007). TNFR1-induced NF-kappaB, but not ERK, p38MAPK or JNK activation, mediates TNF-induced ICAM-1 and VCAM-1 expression on endothelial cells. Cell Signal *19*, 1238-1248.

Ziff, E.B. (1990). Transcription factors: a new family gathers at the cAMP response site. Trends Genet *6*, 69-72.

Wang, T.M., Chen, C.J., Lee, T.S., Chao, H.Y., Wu, W.H., Hsieh, S.C., Sheu, H.H., and Chiang, A.N. (2010). Docosahexaenoic acid attenuates VCAM-1 expression and NF-kappaB activation in TNF-alpha-treated human aortic endothelial cells. J Nutr Biochem. doi:10.1016/j.jnutbio.2010.01.007

附錄

細胞內cAMP濃度測定 (Measurement of intracellular cAMP concentrations)

原理：利用cAMP-acetylcholinesterase (AChE) conjugate (cAMP Tracer) 和樣品中的cAMP互相競爭與cAMP EIA antiserum的結合。反應後移除未結合的cAMP Tracer並加入Ellman's Reagent進行呈色反應。Ellman's Reagent含有AChE的受質，與cAMP Tracer反應後會呈現黃色，可於波長412 nm下讀取其吸光值，最後可依標準曲線計算出樣品的cAMP含量。

實驗操作：EA.hy926細胞處理穿心蓮內酯30分鐘後以冰的PBS洗兩次，加入0.1 N HCl 200 μL於室溫下反應20分鐘。刮取細胞至1.5 mL離心管中混合均勻，以1000×*g*離心10分鐘後吸取上清液。利用Cyclic AMP EIA kit (Cayman Chemical Company, Ann Arbor, MI) 測定細胞內cAMP濃度。取cyclic AMP EIA kit中的96孔盤分別加入50 μL樣品或標準品後依序加入50 μL cAMP AChE Tracer與50 μL cAMP EIA antiserum於4℃下反應18小時。反應結束後以200 μL Wash Buffer清洗五次，加入200 μL Ellman's Reagent於室溫下反應120分鐘。反應後利用ELISA reader測定415 nm下之吸光值，並繪製標準曲線計算出樣品的cAMP含量。另將樣品利用Coomassie Plus protein assay reagent kit進行蛋白質定量，最後將樣品的cAMP含量 (pmol/mL細胞液) 與蛋白質濃度 (mg/mL細胞液) 進行校正，計算出樣品的cAMP濃度 (pmol/mg protein)，並以控制組作為100%

RNA 干擾術 (RNA interference by small interfering RNA of CREB)

原理：藉由雙股 RNA 片段送到細胞內後，被 Dicer 作用分解成小片段 RNA (small interfering RNA, siRNAs)，此雙股的 siRNA 會與 RNA-induced silencing complex (Risc) 產生交互作用形成單股 siRNA 並與目標基因的 mRNA 互補結合。而此互補結合的 RNA 片段會被切下並降解，使得目標基因無法進行轉譯作用，抑制該基因的表現。

實驗操作：人類 CREB siRNA 與 non-targeting control-pool siRNA 購自 Dharmacon Inc. (Lafayette, Colorado)，而人類 CREB siRNA 序列如下：(1) GAGAGAGGUCCGUCUAAUG，(2) UAGUACAGCUGCCCAAUGG，(3) CAACUCCAAUUUACCAAAC，(4) GCCCAGCCAUCAGUUAUUC。當 EA.hy926 細胞培養至八分滿時進行 siRNA 轉染：取三試管，於試管一中加入 OPTI medium100 μL 與 2 μM non-targeting control-pool siRNA 100 μL、試管二中加入 OPTI medium 100 μL 與 2 μM 人類 CREB siRNA 100 μL、試管三則依 3 μL：197 μL 的比例取 DharmaFECT1 transfection reagent 與 OPTI medium 混合，在室溫下反應 5 分鐘後由試管三取出 200 μL 分別加入試管一與試管二中混合，並於室溫反應 20 分鐘。以回溫的 PBS 清洗細胞兩次後分別將試管一與試管二的 mixture 各自加到培養皿中，並補足 2 mL OPTI medium，使欲轉染的 siRNA 最後濃度為 0.1 μM。轉染 8 小時後改以含 10% FBS 的 DMEM medium 預處理穿心蓮內酯 16 小時後再與 TNF-α 共同培養 6 小時，收取細胞蛋白質進行西方墨點法分析蛋白質表現。